The Role of Microtubules and the Centrosomes in Golgi Complex Dynamics and Migration During Interphase

By

Keyada B. Frye

Dissertation

Submitted to the Faculty of the

Graduate School of Vanderbilt University

In partial fulfillment of the requirements

for the degree of

DOCTOR OF PHILOSOPHY

in

Cell and Developmental Biology

August 7, 2020

Nashville, Tennessee

Approved:

Matthew Tyska, Ph.D.

Ryoma Ohi, Ph.D.

Katherine Friedman, M.D.

Todd Graham, Ph.D.

Irina Kaverina, Ph.D.

To my beautifully spirited mother Melodie, who has loved and prayed for me

for my entire life

and

To my siblings, Tamica and Ronald, who are my biggest motivators

ACKNOWLEDGEMENTS

Entering graduate school as a bright eyed twenty-one-year-old, I would have never imagined the journey I was in store for. I've grown so much over the past seven years in more ways than one. Juggling a demanding curriculum and research project, being away from my family in times of happiness and despair, while full time "adulting" undoubtedly required a major learning curve. I put on my big girl pants and made it through. I've finally arrived. I'm so proud of the woman I've become. To my support system, my family, my heartbeats, you all are truly a blessing. My mommy thanks for fighting back and being here today. Tamica, you are my rock. To RJ, Patrick, Melvin, Cynthia, and Elvin, all of my nieces and nephews and my best cousins Crystal, Dee Travis, Bailee, and Pax, thanks for all of the joy, laughter, money (Tamica), and food (Cynthia) over the years. While maintaining long-distance friendships with my some of my favorite people on earth; Lateesha, Rachelle, Antavius, Ciara, Whitney, and Tiffany sometimes proved difficult, we are still going strong and I appreciate the love, support, weekend getaway trips, and pep talks over the years. To all of my doctor friends (PhD, PharmD, MD, MD/PhD); Gaby, Roslin, Léolène, Chris, Rozzy-Reece, Andreia, Miranda, Bianca Islam, Chandan Morris Robbins, and last but certainly not least, my Angelle! I'VE FINALLY JOINED THE CLUB! I'm so grateful to know such a group of intelligent and driven individuals who have gone through this journey with me at Vanderbilt or served as a mentor over the years, dating back to my undergraduate years at Georgia State University. I will forever cherish our relationships. You guys really kept me on my toes! To the leadership (Linda, Roger, and Christina) and my peers within IMSD, thanks for providing a safe space where I could grow as a scientist and work through the issues that arise as being a Black woman at a PWI. I would not have made it without you all. Also big thanks to Dr. Brunson, the VU-Edge program and OBGAPS. To all of my special friends from Georgia State (Yamiece, Jamie, Shalayna, Litany) as well as those I've met here in Nashville (Hamida, Lynette, and Brian)

thanks for being a part of my journey. To my love, Kristen, what we have built in this past year, I never could have imagined it; and where we're going, the best is yet to come.

I would like to acknowledge my advisor, Irina, for being so supportive and loving over the years, for cheering for me and pushing me to my fullest potential as a woman in science. Not only did you win me over with your lively spirit and amazing microcopy, but the diversity you have maintained in your lab is something everyone should strive for. You are the model system. Many thanks to my committee members: Drs. Matt Tyska, Kathy Friedman, Todd Graham, and Puck Ohi. I appreciate your support and pushing me to the finish line. To all of the Kaverina lab members of the past and present, especially Kai, Xiaodong and Anneke; I will forever be grateful for your friendship, scientific expertise, and constructive criticism, moving parties (Kai), and cat stories (Anneke). To my mentee Nivan, I'm so sorry COVID19 stole our final semester to finish the screen! You were a joy to work with and I can't wait to see what cool things you do as you finish your undergraduate career. I'm grateful for the funding and programs available during undergrad with objectives to increase diversity and under-represented PhD candidates, especially in science—Thomas L. Netzel Scholarship, Ronald E. McNair Post Baccalaureate Achievement Program, Louis Stokes Alliance for Minority Participation; as well as my advisors at Georgia State University, Dr. Dixon and Dr. Gilbert, for inciting my love for science. Finally, a special shout out to the ladies in the VU BRET Office of Career Development. The programs you all have organized and guidance you've provided over the years have truly been invaluable.

This work was supported by the National Institutes of Health (NIH) grants R35-GM127098 (to I.K.), R01-DK106228 (to I.K.) and NIH training grant R25-GM062459 "Initiative for Maximize Student Diversity" (Sealy, PI).

TABLE OF CONTENTS

LIST OF FIGURES

Figure Page

CHAPTER I

INTRODUCTION

Cell Cycle Regulation of Mammalian Cells

Across eukaryotic organisms, the concept of a highly regulated process known as “the cell cycle” is highly conserved. The complexity of the molecular machinery which controls this process, as well as the duration of the entire cycle varies according to organism complexity. However, for all living things there is a common core of highly regulated reactions which support the duplication and equal distribution of genetic and cellular material between daughter cells. There are four sequential cell cycle stages; G1, S phase, G2, and M phase. G1, S, and G2 comprise interphase; during M phase cell undergo division and two daughters are formed. During S phase is a key cell stage as this is the time where DNA replication occurs which is required for cells to undergo mitosis in M phase. It is flanked by two gap phases, where cells have time to catch up in growth if necessary. After G2, M phase proceeds first with mitosis, or segregation of genetic material to either pole and finally cytokinesis, which is the physical separation of daughter cells into two units. Cyclin-dependent kinases (CDKs) and their temporal activation by specific cyclins control the cell cycle at several stages; G0/G1 transition, G1/S-phase transition, S-phase progression, G2/M transition, and M-phase progression (Alberts et al., 2002).

CDKs are heterodimeric enzymes which undergo stepwise activation to control the cell cycle (Malumbres, 2014). First, the proper cyclin must bind to an inactive CDK enzyme to induce a conformational change. This reaction must occur for the subsequent phosphorylation of the complex via the CDK activating kinase (CAK) (Pavletich, 1999). The now active cyclin/CDK

complex can phosphorylate a range of substrates depending on the cell cycle stage. While CDK concentrations are steady throughout all stages of the mammalian cell cycle, cyclin levels oscillate to direct the progression to subsequent cell cycle phases. There are several major types of each CDKs (CDK1, CDK2, CDK4, CDK6) and cyclins (A, B, D, E), among others. CDKs are promiscuous and have the ability to bind many of the cyclins. Their localization and higher activity level in one cell cycle stage versus control transition between cell cycle stages. In mammalian cell systems, cyclin D/CDK4/CDK6 controls the G0/G1 transition, cyclin E/CDK2 and cyclin A/CDK2 controls G1/S transition and progression, and cyclin B/CDK1 controls G2/M transition and progression. Negative regulators such as CIP/KIP family of CDK inhibitors (CDKIs) bind and deactivate cyclin/CDK complexes at certain cell cycle transitions to regulate the cell cycle (Humphrey & Brooks, 2004).

Cytoskeleton

The architecture that gives a cell its shape as well supports diverse functions such as cell division, intracellular trafficking, endocytosis, cell migration, and mitigation of outside forces, is a complex system of three filamentous polymers. Microfilaments, intermediate filaments, and microtubules are three classes of the cytoskeleton that offer varying levels of cellular support and function. Microfilaments (actin) are the thinnest of the three polymers (7nm) and are integral in the movement of the cell as a whole, providing mechanical structure and motility. Intermediate filaments are slightly thicker (10nm) and maintain the shape of the cell and support the nucleus by resisting mechanical forces. Finally, microtubules (24nm) are the thickest of the three polymers and support cell division and trafficking of diverse cargos throughout the cell. Each filament type has unique properties and a set of interacting proteins which allow them to function both separately and as an interconnected meshwork supporting vital cellular processes (Fletcher & Dyche Mullins, 2010)

Actin

Actin is a highly abundant and essential component in mammalian systems. It is heavily implicated in providing mechanical support for cellular migration, aid in membrane trafficking to support clathrin-mediated endocytosis (Smythe & Ayscough, 2006), and allows for the physical separation of daughter cells in cytokinesis (Pollard & Cooper, 2009). To support these various functions, there has to be seamless coordination of ATP-actin monomer hydrolysis events, activity of regulatory proteins, and activity of molecular motors of the myosin family to provide contraction forces which is the basis of all of actin based cellular processes.

The structure of microfilaments is comprised of monomers of globular-actin or G-actin which polymerize to become filamentous-actin, or F-actin. G-actin is an ATP-binding protein and like others of this kind, once it is assembled into a filament with other monomers, ATP is hydrolyzed into ADP and an inorganic phosphate (P_i) to produce force (Pollard, 2016). Regulatory proteins then have the ability to bind ADP-actin and control rates of polymerization, turnover, and binding of other regulatory proteins which in turn control actin length and force production capabilities (Pollard et al., 2000). F-actin is polar with a barbed or plus end which undergoes faster polymerization and exerts pushing forces (Huxley, 1963; Woodrum et al., 1975). The pointed or minus end of the filament is not readily capable of generating force. Multiple actin filaments can produce both pushing and pulling forces. Actin organization and localization can determine force capability and function.

In migrating animal cells, actin filaments form several structures localized to the cell front, cell rear, or along the cell body which act in concert to support cellular movement. Two structures which promote protrusion of the cell front are filopodia and lamellipodia. Filopodia are comprised of single, parallel actin bundles with all barbed ends oriented toward the filopodia tip. These finger-like protrusions are oriented at the cell front and act to feel out the environment. On the other

hand, lamellipodia are highly branched actin filaments which span across the entire cell front (reviewed in Svitkina, 2018). Despite such different organizations, both structures are able to support protrusions based upon the same core concept; barbed ends are readily elongated via addition of actin monomers which have been recycled from the pointed end of the filament. This process is known as treadmilling (Neuhaus et al., 1983). The polymerization of these filamentous structures is supported by the regulatory protein Ena/VASP which acts to localize formins, a family of actin binding proteins, to the barbed ends. This reaction leads to highly dynamic filopodia and lamellipodia (Yang et al., 2007). Factors which act to reduce dynamics at the barbed ends, known as capping proteins and retrograde flow of actin must be overcome to support growth. Capping proteins play a major role in branched actin networks to control barbed end dynamics (Zigmond, 2004).

Due to its highly branched structure, lamellipodia barbed end dynamics is more complex than filopodia which primarily only use treadmilling of individual filaments for growth; lamellipodia require a set of regulatory proteins to support and maintain growth. The Arp2/3 protein complex serves as nucleation sites along the actin filament, producing new, “daughter” filaments which grow off the original filament. Branched nucleation can be promoted by the WASp family of proteins. As daughter filaments are born and grow, they also must be capped and their elongation halted. This is necessary to prevent uncontrolled growth or unproductive use of actin monomers. Severing by the protein complex ADF/coflin is a specific negative regulator of branched actin dynamics. Accessory proteins act in protrusion dynamics by promoting crosslinking between actin filaments and serving as linkages between actin and other structures like motors and membranes, at the cell front (reviewed in Svitkina, 2018).

Along the rest of the cell body, actin filaments form specialized structures which contribute to force generation via contraction. Bundling of actin filaments by the protein α-actinin builds

stress fibers which allow for efficient contraction events (Sjöblom et al., 2008). In nonmuscle cells, Myosin IIA is the primary molecular motor that binds to stress fibers to generate force. The powerstroke of this motor depends on ATP hydrolysis of its regulatory light chain (Vicente-Manzanares et al., 2009). Stress fibers are attached at their ends at focal adhesions, which in turn link to the plasma membrane to propagate force generated by myosins and other motors. Focal adhesions are complex structures containing various signaling and adaptor proteins which allow communication inside and outside of the cell to support cell migration (Svitkina, 2018). The family of Rho GTPases include Rac, Rho, and Cdc42 are key regulators of the cytoskeleton. They act by lending the cell spatiotemporal regulation of contraction (Ridley, 2015). All in all, force generation within the cell is transferred to the substrate to allow for cellular locomotion due to the litany of regulatory events which take place.

Intermediate Filaments

The building block of intermediate filaments (IFs) is a coiled coil rod domain flanked by a N-terminal head and a C-terminal tail domain. These monomers increase in complexity as the coiled coil rod allows for lateral associations to form unit length filaments (ULFs) which are eight laterally associated tetramers which additionally undergo compaction which are typical configuration of cytoplasmic IFs. This non-polar configuration does not provide a minus and plus end, therefore IFs do not support motor dependent movement like in other cytoskeletal filaments. Unlike actin and microtubules, which grow via incorporation of ATP- or GTP- bound monomers (see “Actin” and “Microtubule” for details), IFs undergo self-assembly. While it was long thought were not dynamic because of their extreme stability, this notion has recently been dispelled. Actually, IFs are able to rearrange their network similar to the other cytoskeletal polymers (Etienne-Manneville, 2018; Robert et al., 2016). Intermediate filaments can be broadly characterized as either nuclear or cytoplasmic. While lamins, a specific class of intermediate filaments, are associated with nuclear support functions, great diversity lies in IF proteins localized

in the cytoplasm. These proteins can then be grouped into various classes which vary greatly between cell types, functioning to provide a cushion against mechanical force. Overall, the high abundance of IFs and diverse functions reiterates their importance in the cell. Research has continued to uncover more about this elusive polymer.

Microtubules

Microtubules (MTs) are long, rigid, hollow tubes which support diverse vital cellular processes including protein trafficking, motility, locomotion, and mitosis (Goodson & Jonasson, 2018). MTs have a functional subunit of αβ-tubulin heterodimers which align head to tail to form polarized protofilaments. The end at which β-tubulin is exposed is also known as the dynamic plus end, as this is the site where new tubulin subunits can readily be added to the filament. The α-tubulin exposed end of the M is the minus end. In mammalian cells, microtubules contain 13 protofilaments, but it is of note there are other protofilament configurations across model organisms and cell types (Desai & Mitchison, 1997).

While spontaneous nucleation of MTs is neither common nor energetically favorable, it is possible when the concentration of tubulin subunits is in excess. New microtubules are more likely to be nucleated at γ-tubulin containing foci known as γ-tubulin ring complexes (γ-TuRC) which serve as a templates for microtubule growth (Desai & Mitchison, 1997; Evans et al., 1985). These foci are localized at microtubule organizing centers (MTOCs). Centrosomes (Paz & Lüders, 2017) and the Golgi (Chabin-Brion et al., 2001) complex are major MTOCs, as the bulk of all microtubules produced in mammalian cells originate from these organelles. During microtubule polymerization, GTP- tubulin subunits are added to the growing end of the microtubule. The GTP bound □-tubulin is hydrolyzed to become the GDP-tubulin lattice. This polymerization phase may continue until there is a rapid loss of tubulin dimers from the growing end which is defined as catastrophe. Due to this stochasticity of microtubule dynamics, the shrinking microtubule can just

as readily start to regrow in a rescue, via the incorporation of new GTP-tubulin to the plus end. The rapid cycling between polymerization and depolymerization phases of microtubules is known as dynamic instability, which can be modulated by availability of free tubulin (Desai & Mitchison, 1997; Mitchison & Kirschner, 1984).

In a complex eukaryotic system, in addition to free tubulin availability, cells have other means of controlling microtubule dynamics, especially regulation by microtubule-associated proteins (MAPs). There are several classes of MAPs which can be categorized by their localization and/or regulatory activity of stabilization or destabilization of the microtubule. Of course, MAPs localizing at the minus end versus the plus end or lattice might interact with MTs differently, offering an additional layer MT dynamics regulation. Lattice-binding proteins are commonly stabilizers. MAPs which target either end of the MT can also serve to stabilize. One of the most notable MT plus end associated protein families are +TIPs. These proteins track the growing end of the microtubule, so they readily promote polymerization (Akhmanova & Steinmetz, 2008). Other MAPs stabilize MTs by promoting polymerization and/or slowing depolymerization. Finally, there are also specific minus end stabilizing MAPs such as gamma-tubulin ring complex (γ-TURC) and calmodulin regulated spectrin associated protein family member (CAMSAP) (Akhmanova & Steinmetz, 2019; Jiang et al., 2014). On the other hand, there are several MAPs which act to destabilize MTs by severing MTs, sequestering free tubulin, or directly destabilizing the plus end of the MT, such as the depolymerizing kinesin-13 (Desai et al., 1999; Goodson & Jonasson, 2018; Helenius et al., 2006; Hunter et al., 2003).

Microtubule based motors are essential for carrying out the diverse functions of microtubules across the cell. Kinesin motors are usually plus end directed motors which travel along MT tracks to carry cargo. The kinesin family of motors are diverse, differing by their structure and binding ability (Hirokawa et al., 2009). Kinesins comprise of a two-headed motor which uses hand over

hand stepping to traverse the microtubule track and a tail domain typically used for cargo binding. Some kinesins are configured with two motor domains which allow for binding two antiparallel microtubules, as seen in the mitotic Eg5 (Kapitein et al., 2005). This reaction allows for centrosome separation in preparation for mitotic entry. Cytoplasmic dynein is the other family of microtubule motors which solely moves toward the minus end of the microtubule. It also has two motor head domains for walking, but requires accessory proteins such as dynactin and BicD2 for processivity (Reck-Peterson et al., 2018; Splinter et al., 2012).

As it has been mentioned briefly earlier, microtubule function varies across the cell, with a major role occurring in mitosis. At this cell cycle stage, centrosomal microtubules build the mitotic spindle; the structure at which chromosomes are aligned and segregated in mitosis (Gourret, 1995). However, throughout interphase, microtubule functions are notable. MTs give the cell polarity and provide tracks for intracellular transport of organelles and cargo. MTs have inherent polarity and therefore the alignment of these polar elements, specifically with their plus ends oriented toward the cell periphery contributes to whole cell polarity along with actin; providing a cell front and back. The significance of microtubules having their plus ends oriented toward the cell periphery lies in another of its function; providing tracks for the transportation of signaling molecules to focal adhesions to support cell motility. Kaverina et al revealed that MTs target focal adhesions (Kaverina et al., 1998) and, through this contact, that Rho GTPases such as Rac are delivered (see the significance of these reactions in “Actin”) (Kaverina & Straube, 2011). MTs also serve as tracks for other cargos destined for the cell periphery (Hirokawa et al., 2009; Reck-Peterson et al., 2018)

Cell Cycle Regulation of Microtubules

Like all cellular components, microtubules are heavily regulated to ensure cell division with appropriately partitioned genetic material in each daughter cell. Microtubule nucleation needs to

be promoted at specific cell cycle stages for the overall benefit of mitosis. Increased nucleation is notable at G2 since at this point, the cell has two centrosomes, both with nucleation capacity. So inherently, there is an influx or increase of microtubules. Elevated microtubule levels remain at mitotic entry, and reach the very highest nucleation peak at metaphase, in order to support the building of the mitotic spindle (Piehl et al., 2004).

The mammalian mitotic spindle is a complex structure composed of a highly dynamic, highly dense structure; complete with hundreds of thousands of microtubules and nearly one thousand accessory proteins. Specifically, there are around two hundred microtubule associated proteins (MAPs) which fulfill functions in MT nucleation, MT dynamics, and MT bundling to support the construction of the mitotic spindle (Petry, 2016). Essentially, MAP regulation of mitotic microtubules is necessary in the determination of all parameters of spindle formation and maintenance. Typical interphase functions of MAPs (see “Microtubules”) such as TURC, EB1, and others are similar in mitosis. Notably, microtubule motors play an essential role in this cell cycle stage by cross-linking antiparallel microtubules (Kapitein et al., 2005). This microtubule configuration supports the segregation of two sets of genetic material to either pole, a key purpose of mitosis. Additionally, kinetochore microtubules (K-MTs), are a specialized subset of mitotic MTs that bundle together and target kinetochores, which are chromatid attachment sites, for their proper positioning at the metaphase plate (Biggins & Walczak, 2003). There are additional MT subsets which are relevant in mitosis that make up the rest of the spindle (Non-KT MTs) or serve to anchor the spindle in the cytoplasm (astral MTs). Microtubules nucleated at the centrosomes are most readily incorporated into the growing spindle (Petry, 2016). Interestingly, while astral microtubules emanating from the centrosomes contribute an abundance of MT material, it is possible that the Golgi complex (see “Microtubule and Golgi Interaction” below for details) may have some contribution to the astral microtubule array necessary via TPX2 regulation of Golgi membrane nucleation (Wei et al., 2015).

On the other hand, it has been found that GDMTs have a unique cyclic level of nucleation depending on the cell stage, as determined by Maia et al. It was found that Golgi nucleation is at its highest at G2 and prophase while very low throughout the rest of mitosis. These data would suggest that based on nucleating capacity alone, GDMTs do not support spindle assembly or maintenance. At mitotic exit, Golgi-derived microtubules have a spike in nucleating capability (Maia et al., 2013).

Cell Cycle Regulation of Centrosomes

The centrosome is a major microtubule organizing organelle. It is comprised of two centrioles surrounded by pericentriolar material (PCM) which nucleate and anchor radial microtubules. As the cell cycle progress, centrosomes undergo a defined cycle of duplication and maturation in order to produce two centrosomes which will provide a radial array of microtubules to support the mitotic spindle (Fu et al., 2015). Several key kinases facilitate the centrosome cycle progression at each cell cycle stage (G. Wang et al., 2014).

After mitotic exit, mother and daughter centrioles begin the process of disengagement in G1. The cohesin ring complex acts to maintain orthogonal centriole orientation; thus its negative regulation prompts centriole unpairing via activity of the protein separase (Tsou et al., 2009). The mitotic kinases Plk1 and CDK1 activate target proteins to promote these centriole disengagement events. Next, Plk4 directs centriole duplication initiation, near the onset of S-phase. Plk4 recruitment to centrosomes is required for activation of various targets necessary for cartwheel formation (Bettencourt-Dias & Glover, 2007; Kleylein-Sohn et al., 2007). A cartwheel is a structure located on the side of the mother centriole whereby 9 radial spokes radiate which will contact microtubules; its presence is necessary for procentriole formation. Finally, an extensive set of proteins act in concert to stabilize newly formed microtubules, promote centriolar elongation, and

determine final centriole length to overall support procentriole elongation and integrity (Fu et al., 2015).

As a primary function, centrosomes make up the bipolar spindle, and thus need to locate on opposite sides of the cell. First, the proteinaceous linker which joins the two centrosome pairs must be broken. This event, referred to as centrosome disjunction, is initiated in G2 by activation of CDK1 (Fu et al., 2015). C-Nap1 is the major docking protein at the centrosome linker and once it is phosphorylated by CDK1, this protein and all of its interacting proteins are lost, therefore initializing centrosome separation (Fu et al., 2015). A second means of centrosome separation is CDK1 activation of Eg5. Eg5 is a mitotic kinesin motor which tethers non-parallel microtubules. Via its plus end directed movement, Eg5 is necessary, in most species, for pushing centrosomes away from each other (Ferenz et al., 2010; Slangy et al., 1995). As centrosomes separate, their maturation is activated by Plk1. Mature centrosomes have a higher microtubule nucleating capacity. This is in part due to increased PCM assembly prior to mitotic entry which is necessary for adequate spindle formation. Aurora-A is integral in the late stage of G2 as it is a key regulator of mitotic entry, with activation of its targets such CDC25B (which activates CDK1) (Dutertre et al., 2004) and TACC3 (centrosomal adaptor) (Peset & Vernos, 2008) for facilitation of G2-mitosis transition (Macůrek et al., 2008). After the cell has successfully passed through mitotic checkpoints, the centrosome undergoes disengagement where the procentriole is released from the centriole pair. After this Plk1 mediated step, the proteinaceous linker must be re-established. Overall, the aforementioned G1 licensing steps allow for entry into s-phase where duplication can occur, to complete the centrosome cycle (Fu et al., 2015; Tsou et al., 2009).

Golgi Structure and Function

At its core, the Golgi complex functions at the center of the secretory system to receive newly synthesized proteins from the endoplasmic reticulum and modify those proteins for transport to various final destinations. Once seen as a rigid organelle, extensive studies have uncovered the Golgi complex as a highly dynamic membrane system. Regulated interplay of recycling tubular-vesicular elements, Golgi matrix proteins, and Golgi resident enzymes are vital for the maintenance of the organelle's structure and its functionality as a hub for protein trafficking.

Early electron microscopy studies revealed that the Golgi complex is a series of flattened membranes, or cisternae. Groupings of 4-8 parallel cisternae make up Golgi stacks, and in higher eukaryotes, Golgi stacks are interconnected via tubular connections to comprise what we refer to as the Golgi ribbon. Within the Golgi ribbon, both the intra- and inter-stack connections are maintained by several structural Golgi proteins (Farquhar & Palade, 1981; Shorter & Warren, 2002). The Golgi ribbon is proximal to the endoplasmic reticulum (ER): this positioning is integral to the exchange of newly translated proteins from ER to Golgi. These protein cargos are packaged as COPII vesicles at ER exit sites where they can subsequently undergo fusion to form the ER-Golgi intermediate compartment (ERGIC). These pre-Golgi components subsequently become the Golgi complex. The ERGIC is the receiving side of the Golgi complex. The Golgi complex has three compartments which gives the organelle its polarity. The cis-, medial-, and trans-Golgi compartments are defined by their order in the Golgi stack with the cis-Golgi being closest to the ER and trans-Golgi the furthest. Each compartment is defined by the presence of resident enzymes, which add chemical modifications. After traversing the Golgi complex, cargos exit at the trans-Golgi network (TGN) for secretion or recycling (Brandizzi & Barlowe, 2013).

The Golgi Reassembly Stacking Protein GRASP55, located in medial-and trans- cisternae, and GRASP65, located in cis-cisternae, are each PDZ containing proteins. These homodimeric

proteins trans-oligomerize to create linkages between membranes (Barr et al., 1997; Shorter et al., 1999). Via extensive biochemical assays such as RNAi interference of one or both to reduce protein expression, antibody inhibition, and CRISPR/cas9 gene editing, it was determined single depletion of either GRASP protein consistently results in a reduced number of cisternae per Golgi stack, while double depletion results in complete disassembly of the Golgi complex. These data show GRASP proteins are necessary for Golgi integrity (Feinstein & Linstedt, 2008; Puthenveedu et al., 2006; Zhang & Wang, 2016). GRASP oligomerization can occur across cisternae, to allow the intra-stack connectivity that produces the unit of a Golgi stack. Additionally, trans-oligomers can form between stacks, for trans- or inter-stack linkages to support the Golgi ribbon. Pioneering work has implicated GRASP65 as being able to support both cisternal and stack linkages, while GRASP55 is more focused in cisternae linkages. The fission protein CtBP1-S/BARS has also been implicated in ribbon homeostasis by maintaining the tubular connections within the complex (Spanò et al., 1999; Welgert et al., 1999).

Microtubule and Golgi Interaction

The Golgi complex is intimately connected to the cytoskeleton. Specifically, microtubule polymers are necessary for the maintenance of the normal Golgi structure (Thyberg & Moskalewski, 1999) and intracellular trafficking events (Shorter & Warren, 2002). It is consistently shown that, by disrupting microtubules via the use of depolymerization drugs, the Golgi structure is lost (De Brabander et al., 1986). Without intact tubular connections between stacks, Golgi ministacks are scattered throughout the cytoplasm. In a microtubule free state, normal trafficking events are also impaired. In this state, the disrupted Golgi complex can no longer serve as a hub of trafficking and thus the movement of cargo vesicles throughout the secretory pathway is impaired (Thyberg & Moskalewski, 1999). It is no coincidence that the Golgi complex's inherent localization is near a major MTOC such as the centrosome (Shorter & Warren, 2002). Such localization and the input of the Golgi microtubule array support Golgi's dependence on

microtubules. Microtubules from both arrays aid in maintaining homeostatic Golgi structure and post-mitotic Golgi assembly (Hurtado et al., 2011; Miller et al., 2009) and Golgi polarization (Miller et al., 2009; Vinogradova et al., 2012).

Golgi assembly is a microtubule dependent process which require both the centrosomal (cMT) and the Golgi-derived microtubule (GDMT) array. GDMTs facilitate the dynein-dependent clustering of Golgi ministacks toward each other at the periphery of the cell. Subsequently, cMTs facilitate the inward movement of intact Golgi stacks toward the center of the cell. GDMTs specifically contribute to classic, extended Golgi continuity in its ribbon form; when GDMTs are absent, cMTS cluster Golgi mini-stacks from the periphery back toward the centrosome at the cell's center (Miller et al., 2009). Contributions of both cMTs and GDMTs are also needed for the proper Golgi stack polarity (Hurtado et al., 2011; Miller et al., 2009; Vinogradova et al., 2012).

The Golgi Cycle

The Golgi complex must undergo fragmentation as an essential step prior to mitosis. Extensive studies have been completed to uncover how the organelle undergoes several steps of fragmentation. In preview, the major steps of Golgi fragmentation include Golgi ribbon unlinking, Golgi cisternae unstacking, and vesiculation.

Primarily, *in vitro* approaches were used to conclude that the phosphorylation state of GRASP family proteins modulates Golgi ribbon unlinking and unstacking steps of Golgi fragmentation. In late G2, mitotic kinases such as Cdk1, Plk1, and MEK1/ERK begin to act upon downstream targets. Cdk1 and Plk1 target GRASP65 (Tang et al., 2012; Tang & Wang, 2013), while MEK1/ERK targets GRASP55 (Duran et al., 2008; Feinstein & Linstedt, 2008; S. A. Jesch et al., 2001). In both situations, the phosphorylation of GRASP55/65 causes a loss in dimerization

between cisternae (GRASP55/65) and stacks (GRASP65), resulting in a fragmented Golgi complex.

Additionally, use of confocal microscopy to analyze fluorescent recovery after photobleaching (FRAP) was used to test Golgi fragmentation. FRAP is a process whereby a fluorescent protein of interest is exposed to high levels of laser power, causing photobleaching, or loss of signal (Axelrod et al., 1976; Koppel et al., 1976). However, because of the highly dynamic nature of the Golgi, proteins are quickly recycled, therefore the presence of the protein should return after a determined amount of time, evident by a return of fluorescence signal in FRAP assays (Lippincott-Schwartz & Patterson, 2003). CtBP1-S/BARS dependent Golgi morphology and continuity was spelled out in this way. By inhibiting BARS, the normalized FRAP values of a trans-Golgi marker reflects no fluorescence recovery, indicative that BARS is essential for the maintenance of the Golgi complex (Colanzi et al., 2007).

CDK1 has an additional role in the mitotic Golgi fragmentation scheme. Its phosphorylation of the Golgi matrix protein GM130 prompts advanced Golgi fragmentation from cisternae to vesicles (Lowe et al., 1998). GM130 is a Golgi matrix protein that is located at the cis-Golgi (Shorter & Warren, 2002). It can directly bind the vesicle tethering protein p115 (Nakamura et al., 1997), which mediates ER-Golgi trafficking via binding COPI vesicles (Sönnichsen et al., 1998). P115 also been shown to directly bind giantin (Sönnichsen et al., 1998). Therefore, p115 is recruited to membranes where it can interact with the Golgi proteins giantin and GM130. The GM130-p115 interaction is also notable because GM130 itself can interact with GRASP65, a cis-Golgi localized protein (Barr et al., 1997). In interphase, these active connections allow for homeostatic membrane tethering events. It is only at the onset of mitosis when CDK1 is active, which in turn phosphorylates p115 that this trio is untethered. This state leads to COPI

vesicle budding from the Golgi and the highly vesiculated state of Golgi membranes at mitosis (Y. Wang et al., 2008).

There has been strong support in favor of a “Golgi mitotic checkpoint” (Corda et al., 2012; Hidalgo Carcedo et al., 2004; Sütterlin et al., 2002). This checkpoint is defined by the necessity of Golgi fragmentation to allow for mitotic entry. Extensive *in vitro* and *in vivo* assays have been developed to study the concept of this checkpoint. Ultimately, several groups have found that the loss of Golgi continuity via discontinuity of the Golgi ribbon must occur prior to mitotic onset. More recently, groups implicate the spatial dissociation of the Golgi and centrosome as a key step prior to Golgi fragmentation and subsequent mitotic entry (Guizzunti & Seemann, 2016; Tormanen et al., 2019).

Cell Cycle Regulation of Cellular Motility

Cellular motility is essential in living cells. Whether in normal processes such as collective cell migration at differentiation, movement of immune cells to sources of infection, or abnormal migration of malignant cells, cell migration is a highly regulated process. In the context of this section, cell migration encompasses the cell cycle dependent regulation of focal adhesion complexes by the cytoskeleton to promote displacement of normal cells across substrates. As expanded upon earlier (see “Cell Cycle Regulation of Mammalian Cells”), the progression of the mammalian cell cycle is highly regulated by an elegant system of cyclin dependent kinases (CDKs) and cyclins. Oscillating levels of distinct active CDK/cyclin pairs at specific stages in the cell cycle allow for the transition from G1 to S-phase, to G2, and finally mitosis.

There are several factors that can contribute to migration dynamics. The proper positioning of microtubule organizing centers, such as the Golgi complex and the centrosome at the front of the cell supports delivery of signaling molecules needed for cell migration.

Additionally, changes in how the cell contacts the substrate (the ECM) can determine cell migratory capabilities. More specifically, the increasing levels of CDK1 at mitosis affect cell adhesion turnover, and thus the ability of the cell to migrate (Jones et al., 2018). Various studies corroborate that the Rho family of GTPases can regulate cell cycle progression mainly through controlling the actin cytoskeleton as discussed earlier (see “Actin”) (Ridley, 2015). Interestingly, this family can also activate cell cycle signaling proteins, especially in early cell cycle stages. As it is known, cyclin D1 drives the G1-S transition, and therefore needs to be activated early in this cell cycle stage. Rho, Rac, and Cdc42 have all been implicated in stimulating cyclin D; with Rho specifically activating ERK signaling (Welsh et al., 2001). As CDK1 activity increases, so does adhesion complex size (Jones et al., 2018). This large adhesion complex translates to requiring more energy to turnover, therefore slower migratory speeds. Additionally, when there are increased levels of the mitotic cyclin B, there is a marked decrease in adhesion size and subsequent rounding of cell to loss of adhesion. This decrease directly correlates to the decrease of CDK1 activity at mitosis (Jones et al., 2018).

Thesis Summary

To date, there is an extensive body of research focused on various behaviors of the Golgi complex. Early studies primarily focused on the highly regulated process of Golgi ribbon disassembly, which occurs in late G2 phase through mitosis. These *in vitro* and *in vivo* studies have led to the concept of “the Golgi mitotic checkpoint,” whereby Golgi fragmentation must occur for proper mitotic entry. However, details surrounding Golgi dynamics prior to the onset of fragmentation is lacking. The work presented here introduces several new means to characterize dynamics of Golgi morphology throughout all interphase substages.

In Chapter II, I elegantly utilize high quality, three-dimensional, confocal live-cell imaging to investigate Golgi dynamics at interphase. I have identified three distinct Golgi configurations

that are prevalent in G1, S phase, and G2 phases. I survey the localization and shape of the Golgi complex and quantitate parameters to describe the Golgi in each cell cycle stage and subsequently each Golgi mode that I have defined. In particular, by highlighting the relation of the Golgi and centrosome throughout these stages, I was able to determine a correlation between the timing of Golgi-centrosome dissociation and centrosome separation in interphase. Additionally, I modulate the presence microtubules in the cell to determine how Golgi configurations are altered based on interphase stage. Specific modulation of centrosomal microtubules is also assayed in Chapter II. Finally, I measure the migratory capacity of the cell in each of the defined Golgi configuration modes. Overall, this thesis work is fundamental in providing an analytical means to determine Golgi morphology, Golgi dynamics, and Golgi-centrosome association throughout interphase substages.

CHAPTER II

Cell-cycle dependent dynamics of the Golgi- centrosome association in motile cells

This chapter is published under the same title in *Cells,* April, 2020 (Frye et al., 2020).

Frye, K., Renda, F., Fomicheva, M., Zhu, X., Gong, L., Khodjakov, A., & Kaverina, I. (2020). Cell Cycle-Dependent Dynamics of the Golgi-Centrosome Association in Motile Cells. *Cells*, *9*(5), 1069. https://doi.org/10.3390/cells9051069

Abstract

Here, we characterize spatial distribution of the Golgi complex in human cells. In contrast to the prevailing view that the Golgi compactly surrounds the centrosome throughout interphase, we observe characteristic differences in the morphology of Golgi ribbons and their association with the centrosome during various periods of the cell cycle. The compact Golgi complex is typical in G1; during S-phase, Golgi ribbons lose their association with the centrosome and extend along the nuclear envelope to largely encircle the nucleus in G2. Interestingly, pre-mitotic separation of duplicated centrosomes always occurs after dissociation from the Golgi. Shortly before the nuclear envelope breakdown, scattered Golgi ribbons reassociate with the separated centrosomes restoring two compact Golgi complexes. Transitions between the compact and distributed Golgi morphologies are microtubule-dependent. However, they occur even in the absence of centrosomes, which implies that Golgi reorganization is not driven by the centrosomal microtubule asters. Cells with different Golgi morphology exhibit distinct differences in the directional persistence and velocity of migration. These data suggest that changes in the radial distribution of the Golgi around the nucleus define the extent of cell polarization and regulate cell motility in a cell cycle-dependent manner.

Introduction

The Golgi complex serves as a major hub for intracellular trafficking, allowing for the proper processing of newly synthesized proteins, their sorting, and transport toward proper destinations. The complex comprises polarized stacks of flattened cisternae, which receive proteins translated within the endoplasmic reticulum (ER) at the *cis* face. After traversing through the Golgi stack and acquiring proper modifications, processed proteins are sorted into post-Golgi carrier vesicles that are primarily targeted for transportation toward the plasma membrane. Due to its vital role in protein trafficking, organization of the Golgi has been studied extensively and the consensus is that the localization and morphology of the Golgi is governed by the cytoskeleton. This governance allows for highly dynamic changes in the organization of Golgi that are paramount for the proper function of this organelle.

In higher eukaryotes, Golgi stacks are linked via tubular connections into a Golgi ribbon whose integrity is important for its role as the central protein processing and sorting station. The integral Golgi complex exists during interphase but must fragment as the cell enters mitosis (J. M. Lucocq & Warren, 1987; Shima et al., 1997; Sütterlin et al., 2002). Fragmentation involves a breakdown of the Golgi ribbon into individual stacks (Colanzi et al., 2007), unstacking and vesiculation of Golgi cisternae (Misteli & Warren, 1995), and cycling of Golgi components through the ER (Stephen A. Jesch et al., 2001; Sengupta et al., 2015). The fragments accumulate near spindle poles organized by the centrosomes which ensures proper partitioning of Golgi fragments into the daughter cells (Wei & Seemann, 2009).

Upon mitotic exit, multiple stacks re-emerge and rapidly re-assemble into the Golgi ribbons in daughter cells (J. Lucocq et al., 1989). This reassembly is facilitated by transport of ER-to-Golgi carriers and Golgi stacks toward the minus ends of microtubules (MTs) (Burkhardt et al., 1997; Thyberg & Moskalewski, 1999), driven by the minus-end directed molecular motors dynein

(Harada et al., 1998; Ríos et al., 2004; Vaisberg et al., 1996) and KIFC3 (Xu et al., 2002). Transport of Golgi elements relies on two subpopulations of MTs: Golgi-derived MTs are engaged in the transport of Golgi stacks towards each other and are necessary for the ribbon integrity (Miller et al., 2009; Vinogradova et al., 2012) while the radially organized MTs produced by the centrosomes collect Golgi membranes to a common complex in the vicinity of the centrosome. The centrosome is the most efficient cellular MT-organizing center (MTOC), thus MT minus end concentration is the highest here. As a result, the assembled Golgi ribbon is found closely associated with the centrosome. Additional direct molecular links between the Golgi and centrosomes also support association of those organelles (Rios, 2014; Tormanen et al., 2019).

In post-mitotic cells, the centrosomes define the location of the Golgi via these mechanisms. Golgi positioning plays a critical role in cell polarity (Farhan & Hsu, 2016)(Ravichandran et al., 2020), which is particularly important in polarized cells that export post-Golgi proteins in a single defined direction. Such cells position the Golgi near the destination point of secretion. For example, the Golgi is proximal to the apical surface in polarized epithelia that secrete apically (Weisz & Rodriguez-Boulan, 2009). In directionally migrating mesenchymal cells, Golgi resides between the nucleus and the protruding edge, supporting the front-directed Golgi-derived MT array and the transport of the building material to the protruding edge (Miller et al., 2009; Prigozhina & Waterman-Storer, 2004; Yadav et al., 2009). The centrosome is thought to drive proper positioning of the Golgi in this context (Sütterlin & Colanzi, 2010).

Although the morphological and functional partnerships between the Golgi and the centrosome appear to be well established, noteworthy is that Golgi assembly and its location location have been primarily assessed in early G1, soon after the cell exited mitosis or in quiescent differentiated cells that have exited from the cell cycle into G0. Morphology and behavior of the Golgi as well as its connections with the centrosome throughout interphase in actively proliferating

cells have not been detailed. In this study, we follow the dynamics of Golgi and centrosome positioning throughout the cell cycle in highly motile and rapidly growing RPE1 cells. By combining 3-D live-cell time-lapse imaging and quantitative fixed population analyses, we characterize dramatic cell-cycle-dependent changes in the localization and morphology of the Golgi ribbon as well as the association of the Golgi and centrosome. We also demonstrate that these dynamic Golgi rearrangements strongly influence the efficiency of polarized cell migration during various phases of the cell cycle.

Results

Morphology of the Golgi Complex and Its Association with the Centrosome Varies Depending on the Cell Cycle Stage

Analysis of the Golgi morphology and its association with the centrosome in fixed cells randomly selected from asynchronous populations of human euploid RPE1 line suggests prominent cell-cycle specific differences in the organization of this organelle. To identify cells during various phases of the cell cycle, we briefly expose RPE1 cells that constitutively express a GFP fusion of centriolar protein Centrin-1 (Lončarek et al., 2010) to BrdU. In this approach, nuclei of cells in the S phase become labeled due to incorporation of BrdU while G1 and G2 cells remain unlabeled (Figure 1a). The latter stages are discriminated by the organization of the centrosome as G1 cells contain two individual centrioles while G2 cells display two centriolar doublets (diplosomes) (Figure 1a) (Lončarek et al., 2010; Piel et al., 2000). Prophase was identified as the period when the condensed chromosomes within the intact nucleus can be morphologically detected (Figure 1a). In an alternative approach, we employ Fluorescent Ubiquitination-based Cell Cycle Indicator (FUCCI (Sladitschek & Neveu, 2015)) (Figure 1b). Both approaches yield similar results. Consistent with previous reports (Miller et al., 2009; Presley et al., 1997), the Golgi appears compact and closely associated with the centrosome in G1 cells. In

contrast, Golgi-centrosome association is not apparent at later stages of the cell cycle (Figure 1a).

To quantify spatial proximity of the centrosome to the Golgi, we employ the mean of distances between the centriole and each of the voxels within segmented volumes of the Golgi (Golgi-Centrosome distance, GC, Figure S1a). GC values are low in G1 phase but higher and more variable among S-phase cells (Figure 1c). These differences indicate that the Golgi spreads away from the centrosome as the cell progresses through S-phase. Morphologically observed increases in GC values correspond to Golgi extension along the nuclear envelope (Figure 1a, 'S' and 'G2'), which we describe as the 'equatorial' or 'E mode' configuration. In cells with equatorial Golgi, the centrosome tends to separate from the Golgi ribbons and assume position closer to the center of the nucleus either at its ventral or dorsal surface (Figure 1a, 'S'). In G2, GC values are consistently high, while the centrosome remains detached from the equatorially distributed Golgi (Figure 1a, 'G2'). In prophase cells, GC values decrease as the Golgi appear to re-associate with the centrosomes that continue to reside beneath or above the nucleus near its center (Figure 1c).

We use two parameters to numerically assess changes in Golgi morphology: Golgi-to-Golgi index (GG) and percent of equatorial redistribution (PER). The former reflects the extent of Golgi fragmentation and scattering and is calculated as the mean of pairwise distances among all voxels within the segmented volume of the Golgi (Figure S1a). The latter is proportional to the extension of the Golgi around the nuclear equator and is measured as the percent of the nuclear perimeter that is in close proximity with the Golgi (Figure S1a). We observe a strong correlation between the values of GG and PER during all cell-cycle phases (Figure S1b) allowing us to use either type of analysis as needed.

We find that in G1 both metrics are low (Figure 1d,e) consistent with the observed compact morphology of the Golgi. Henceforth we will reference this quantifiable morphology as Compact configuration mode-1 (C1 mode). Interestingly, we find a strong direct correlation between the metrics describing Golgi-centrosome association (GC) and Golgi scattering (GG) during G1, supporting the idea that collecting the Golgi around the centrosome is an important factor in Golgi compaction in G1 cells (Figure 1f).

In S-phase and G2, GG and PER values progressively increase, as many cells reach the extended Golgi configuration (E mode) (Figure 1d,e). However, variance of both metrics is high in S-phase consistent with the visually observed variability of Golgi morphology and centrosome configurations (Figure S2). It is not uncommon to observe S-phase cells with centrosomes spatially separated from compact Golgi complexes (Figure S2c). Conversely, on occasion the Golgi is found in E mode while the centrosome resides adjacent to Golgi ribbons (Figure S2b). Consistent with these observations, only weak correlation between GC and GG is observed for S-phase cells (Figure 1f'). This variability suggests that centrosome detachment and early stages of Golgi equatorial spreading are roughly coincidental but not necessarily interdependent. In G2, when the Golgi is in E mode, the correlation between GG and GC is not detected (Figure 1f"), indicating that the Golgi and the centrosome positioning become completely independent from each other.

In prophase cells, as the Golgi undergoes pre-mitotic fragmentation, the mean value of GG remains similar to that observed in G2 cells (Figure 1d). In contrast, the mean value of PER decreases (Figure 1e). This decrease reflects a change in the spatial distribution of Golgi fragments, which becomes pronouncedly three-dimensional. While in S and G2 cells the Golgi spreads around the nucleus primarily in the medial plane, during prophase a number of Golgi fragments reside beneath and/or above the nucleus on its ventral and dorsal surface (Figure S2e-

h). Interestingly, GG and GC values correlate strongly in prophase cells (Figure 1f"'), suggesting that the activity that collects the Golgi at the centrosomes is restored akin the G1 configuration. Indeed, in a subpopulation of prophase cells the Golgi, while highly fragmented, accumulates in the proximity of the separated centrosomes (Figure S2h and low GC in Figure 1c). This configuration will be referred to as Compact-2, or C2 mode.

Overall, fixed-cell analyses allow us to postulate the existence of three Golgi configuration modes (Figure 2a), indicating that centrosome-associated compact Golgi, thought to be typical for all interphase cell (Colanzi et al., 2003; Thyberg & Moskalewski, 1999), is rarely observed during S and G2 phases.

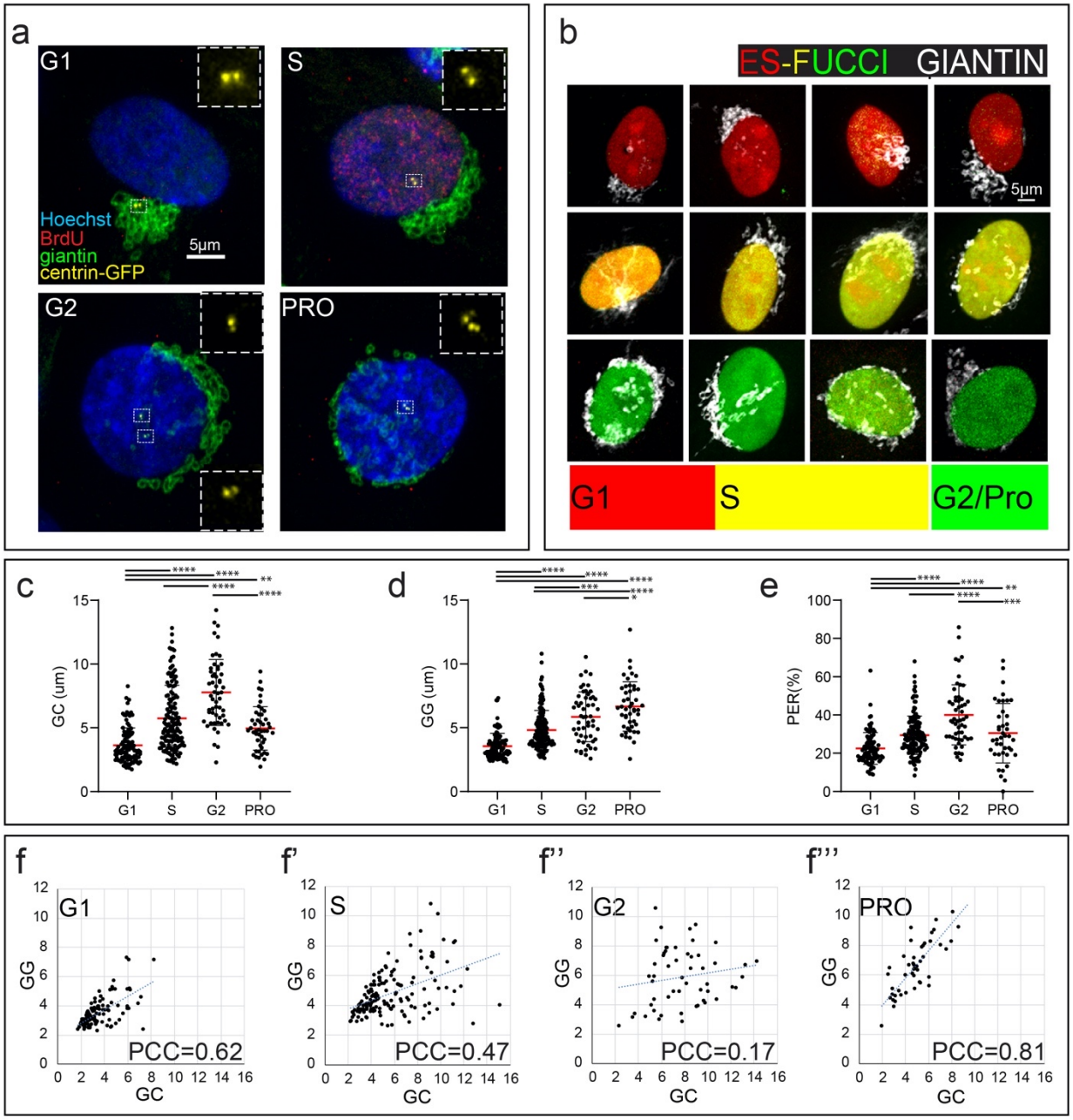

Figure 1. Golgi configuration and centrosome association are cell cycle-dependent.

(a) Representative images of Golgi and centrosome positioning in specific cell cycle phases (G1, S, G2, prophase (PRO). Immunostaining: Hoechst (blue), centrin1-GFP (yellow), BrdU (red), giantin (green). Boxed regions (centrosomes) are enlarged in insets. Maximum intensity projections of laser scanning confocal stacks. Scale 5μm.

(b) Representative images of Golgi (immunostained, giantin, white) throughout the cell cycle as highlighted by ES-FUCCI cell cycle indicator. FUCCI color code: G1, red; S, yellow, G2 and prophase, green). Maximum intensity projections of spinning disk confocal stacks. Scale 5μm. (c–e) Quantification of Golgi and centrosome distribution indices in the fixed cell population based on data as in (a). n = 343 cells total, six experiments. Error bars, SD. Mean, red line. One-way ANOVA with Tukey's multiple comparison test. **** $p < 0.0001$; *** $p < 0.001$; ** $p < 0.01$; * $p < 0.05$. (c) GC (mean Golgi-centrosome distance in 3D space). (d) GG (mean Golgi scattering index in 3D space). (e) PER (percent of equatorial Golgi redistribution). (f-f''') Scatter plots of GG vs GC in cell cycle substages. Pearson correlation coefficients demonstrate positive correlation for GG vs. GC in cell stages G1 (f) and prophase (f''').

Golgi Configuration Dynamics Is Governed by the Cell Cycle Progression

To characterize dynamics of Golgi-centrosome relationships and transitions between the compact and spread configurations of the Golgi we employ 3-D live-cell time-lapse imaging of cells stably co-expressing Centrin1-GFP (centrosome marker) and RFP-TGN (Golgi marker). Initial spreading of the Golgi along the nuclear equator roughly coincides with the centrosome detachment from the Golgi (Figure 2b-b', Movie 1) and this spreading steadily advances until full equatorial extension (E mode) is achieved (Figure 2c-c', Movie 1). The raise in GC values precedes that in GG suggesting that Golgi decompaction follows its dissociation from the centrosome (Figure 2f-f',g). Consistent with our fixed-cell analyses (Figure 1b, Figure S2e-h), shortly before cell division the Golgi is seen accumulating around the separated centrosomes (C2 mode; Figure 2d-d', Movie 1) and the GC value decreases (Figure 2f, arrows). Live-cell recordings also reveal a transient change in the compactness of Golgi prior to cell division (Figure 2f',

arrows). During this change, GG values decrease quite rapidly which makes detection of this transient pre-mitotic compaction difficult in fixed-cell population analyses. Importantly, the GG decrease occurs with a slight delay after the decrease in GC (Figure 2g-g') indicating that the movement of the Golgi toward the centrosome precedes compaction of the Golgi.

To precisely time C2 mode with respect to the NEB (onset of cell division) we correlate dynamics of the Golgi reorganization with redistribution of mCherry-NLS from the nucleus into the cytoplasm (Figures 2h-i, Movie 2). In 7 of 8 recorded cells, the directional movement of Golgi fragments toward the centrosomes is detected prior to the increase in nuclear envelope permeability (Figure 2h, i), suggesting that transition to C2 mode is driven by prophase-associated mechanisms. Upon completion of cell division, the Golgi acquires compact morphology around the centrosome as manifested in the low values of GG and CG characteristic of G1 phase of the cell cycle (C1 mode, Figure 2e-e', f-f', Movie 1).

Overall, live-cell microscopy illustrates dynamic nature of the three Golgi modes, and reveal that transition from C1 to E mode occurs during S phase, E- to C2 mode transition takes place during late prophase, and the compact C1 mode Golgi is assembled coincidentally with mitotic exit.

Figure 2: Dynamics and timing of Golgi configuration modes in living cells

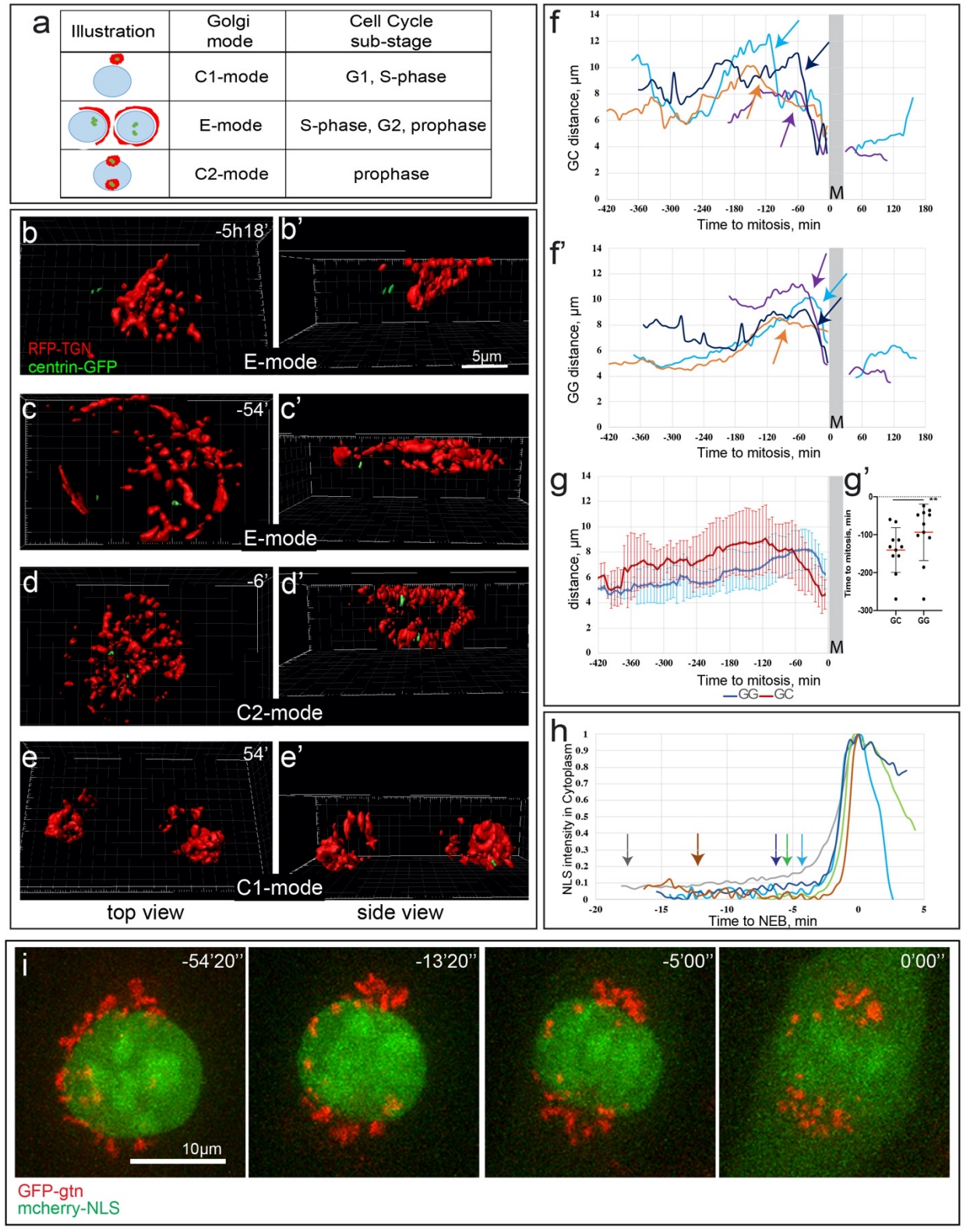

(a) Dynamics and timing of Golgi configuration modes in living cells. (a) Model of Golgi mode progression aligned with cell cycle progression. (b–e') Frames from a time-lapse imaging sequence of RPE1 cells stably expressing Golgi (RFP-TGN, red) and centrosome markers (centrin1-GFP, green). Corresponding Golgi configuration modes: C1-E transition (b,b'), E (c,c'), C2 (d,d'), C1 (e,e'). 3D reconstructions of spinning disk confocal stacks (top-down views (b–e) and side views (b'–e')). Time, hours, minutes. (f) GC and (f') GG distance profiles for 4 representative cells over time. Time point "0" indicates the beginning of cell division. (g) Averaged GC (red) and GG (blue) profiles over time. Sequences aligned by the beginning of cell division (time point "0"). *n* = 9. Error bars, SD. Note the declines of the curves prior to cell division. (g') Time when GC (left) and GG (right) reach maxima before beginning to decline prior to cell division. Data for individual cells analyzed in (g). Note that GC peak is significantly earlier than GG. *n* = 9. Error bars, SD. Student's *t*-test, ** $p < 0.01$. (h) Intensity profiles for NLS signal in the cytoplasm of individual cells prior to and during nuclear envelope breakdown. Based of imaging as in (i). C2 mode onset times are indicated by arrows. *n* = 5. (i) Frames from a time-lapse imaging sequence of RPE1 cells transfected with GFP-gtn (pseudo-colored red) and mCherry-NLS (pseudo-colored green). Note Golgi compaction at -13′20″ and -5′00″ and NLS leakage into the cytoplasm at 0′00″. Scale bar, 10 μm. Time, minutes, seconds. Images are maximum intensity projection of entire spinning disk confocal stacks.

Transition from Compact to Equatorial Golgi Configuration Requires Microtubules but Not Centrosomes

Live-cell recordings indicate that the centrosomes detach from the Golgi during the C1 to E mode transition. To evaluate whether the centrosome plays an active role in this process, we

utilize a PLK4 inhibitor Centrinone known to prevent centriole duplication (Wong et al., 2015). Due to dilution of non-duplicating centrioles in the consecutive cell-cycles, many cells in the population bear a single centriole or lack this organelle completely after 72 hours of Centrinone treatment (Wong et al., 2015). We find that acentrosomal cells undergo normal transition to E mode Golgi (Figure 3a-a', Movie 3 vs. 3b-b', Movie 4) as evident from similar values of GG and PER in centrosomal vs. acentrosomal cells (Figure 3c). Thus, the centrosome and by inference MTs organized by this organelle are not required for C1 to E mode Golgi transition.

Lack of dependency on the centrosome-organized astral MT array suggests that E mode Golgi movements rely on non-radial perinuclear MTs that wrap around the nucleus and are closely associated with the extended Golgi (Figures 3e-e''). Consistent with this notion, rapid directional sliding of Golgi tubules along the nuclear perimeter is often observed in live-cell recordings (Figure 3f, Movie 5). Such fast directional movements are typical for active MT-dependent transport (Welte, 2004). To test whether MTs indeed serve as tracks for E mode Golgi distribution, we utilize cold treatment that leads to MT depolymerization without Golgi dispersion (Minin, 1997; Turner & Tartakoff, 1989), and follow the Golgi dynamics for 30 minutes at 37°C in the presence of DMSO (Figures 3g-g', Movie 6) or nocodazole (Figures 3h-h', Movie 7), which prevents MT reassembly. In the absence of MTs, Golgi scattering occurs as expected (Turner & Tartakoff, 1989) but directional Golgi movements as well as progression towards E mode are blocked as manifested in lower PER values in three independent image sequences (Figure 3d). This indicates that the C1 to E mode Golgi redistribution, while not centrosome-dependent, is driven by MT-dependent transport

Figure 3. Golgi stretching around the nucleus is centrosome-independent and microtubule-dependent.

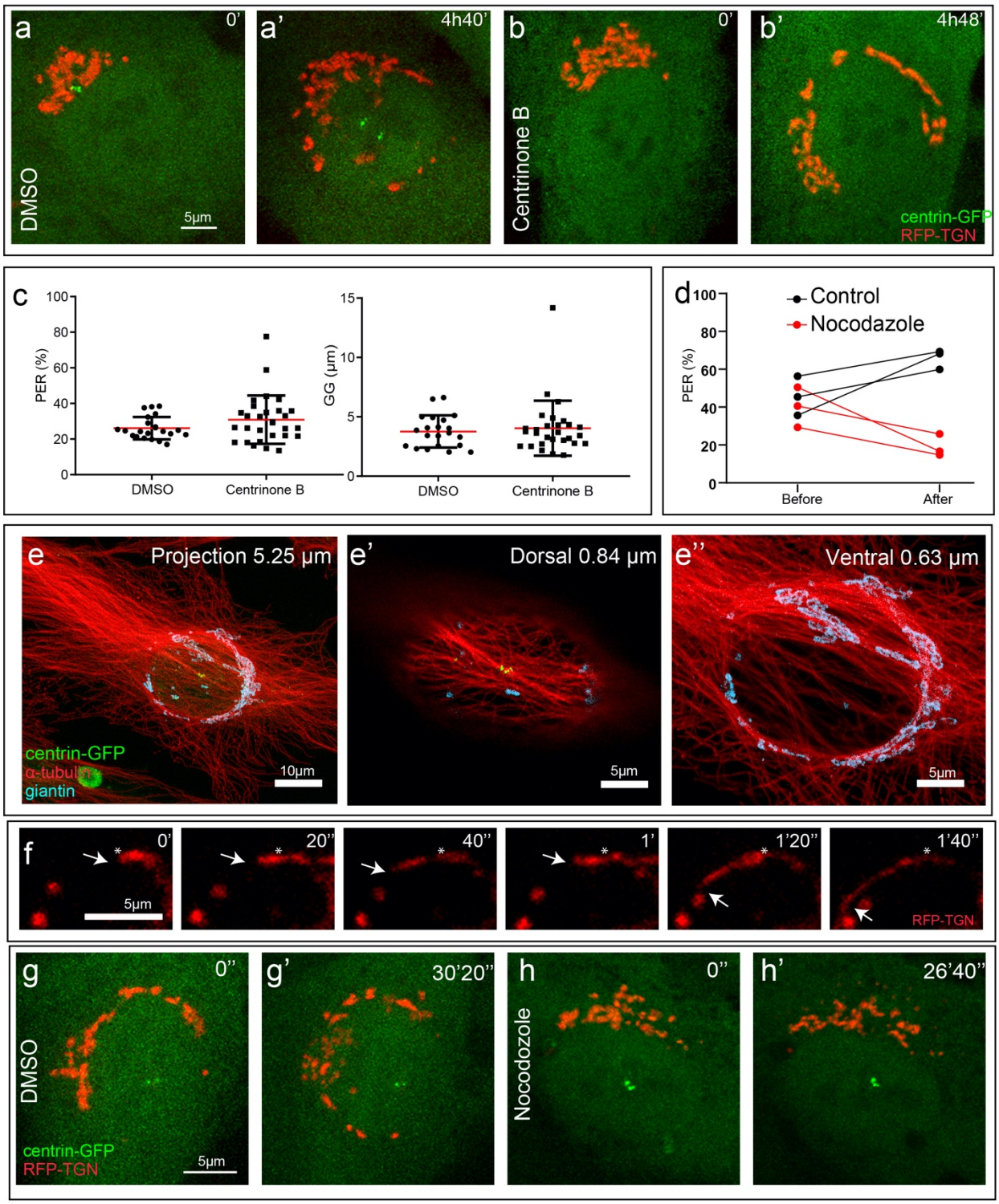

(a-b') Frames from a time-lapse imaging sequence of RPE1 cells stably expressing Golgi (RFP-TGN, red) and centrosome markers (centrin1-GFP, green). E mode progression over 5 hours in (a) control cell or (b) cell pre-treated by Centrinone B for 72 hours. Scale 5 μm. (c) Quantification of PER and GG in fixed S-phase cells (BRDu-positive) pre-treated with DMSO or Centrinone B for 72 hours. Student t-test showed no significant differences between DMSO and Centrinone B-treated cells for either PER or GG. n= 49. Error bars, SD. Red line, mean. (d) Change of Golgi extension during 30 minutes live-cell imaging of cells with and without MTs. Cells pre-treated on ice for 45 minutes were recorded in the presence of DMSO (control) vs nocodazole. PER index before and after imaging is shown. n=3. (e-e'') Localization of the Golgi (giantin, cyan) and MTs (α-tubulin, red) in E mode, immunostaining, centrin1-GFP (green). (e) Cell overview shown as a maximum intensity projection of entire laser scanning confocal stack (5.25 μm-thick). Scale 10 μm. (e'-e") Maximum intensity projections of dorsal (0.84 μm-thick) and ventral (0.63 μm-thick) sub-stacks of the central cell area. Scale 5 μm. (f) Progressive movement (white arrows) of dynamic Golgi tubule (TGN, red) along the nuclear equator shown in 20 second intervals. Asterisk denotes starting position of Golgi membrane tubule movement. Scale 5 μm. Time, minutes, seconds. (g) Live cell visualization of E mode progression in cells pre-treated on ice for 45 minutes and recorded in the presence of DMSO (g) or nocodazole (h, as quantified in d). Golgi (RFP-TGN, red). Centrosome (centrin1-GFP, green). Scale 5 μm. Time, seconds. Images in (a,b,f,g,h) are maximum intensity projection of entire spinning disk confocal stacks.

Golgi Compaction Does Not Require Centrosomes

Our data reveal that compaction of the Golgi occurs twice during a cell cycle: first, upon mitotic exit in G1 and second, during prophase shortly before the NEB. In both cases, the Golgi appears to compact around the centrosome and it is well documented that Golgi stacks are brought together by a MT minus-end-dependent transport (Lippincott-Schwartz, 1998) with both centrosomal and Golgi-derived MTs serving as tracks for Golgi assembly (Miller et al., 2009; Vinogradova et al., 2012). This prompted us to test whether centrosomes play an active role in the transitions to C1 and C2 mode of Golgi.

To test whether the centrosome and centrosomal MT aster are required for proper Golgi compaction, we compare dynamics of transitions to C1 and C2 mode in cells with normal centrosomes (Figure 4a, Movie 8) vs. cells lacking centrosomes (Figure 4b, Movie 9) vs. cells with a single centriole (Figure 4c, Movie 10). Surprisingly, we observe neither a significant difference in Golgi organization (Figure 4a-c, ~30 min time point), nor a significant change in the mean GG value (Figure 4d-d', C1, C1+30min) in centrosomal vs. acentrosomal cells shortly after mitotic exit. Thus, the centrosome and centrosomal MT asters are not required for Golgi compaction during mitotic exit which suggests that non-centrosomal MTs are sufficient for transport of Golgi fragments toward one another at this stage. However, the Golgi in acentrosomal cells becomes decompacted earlier than in control (compare time points "C1+5h" in Figure 4d and Figure 4d'), and a premature redistribution of the Golgi to equatorial configuration is observed in a subset of acentrosomal cells (compare centrosomal vs acentrosomal daughter cells in Figure 4c, 5h36'). This indicates that the compact Golgi is somewhat unstable in the absence of centrosomes consistent with a decrease in Golgi integrity reported previously for acentrosomal cells (Vinogradova et al., 2012).

Similarly, transition to C2 mode during prophase occurs efficiently in acentrosomal cells (Figure 4e-g). As in the presence of centrosomes (Figure 4f, Movie 11), two distinct Golgi clusters form on the dorsal and ventral sides of the nucleus when the centrosomes are absent (Figure 4g, Movie 12). Normal extent of pre-mitotic compaction in the absence of centrosomes is evident from similar sharp decreases in GG values in centrosomal vs. acentrosomal cells (Figure 4e-e'). We therefore conclude that the mechanism(s) driving both C1 and C2 modes do not require centrosomes or radial MT arrays formed by these organelles.

Figure 4. Golgi compaction is centrosome-independent.

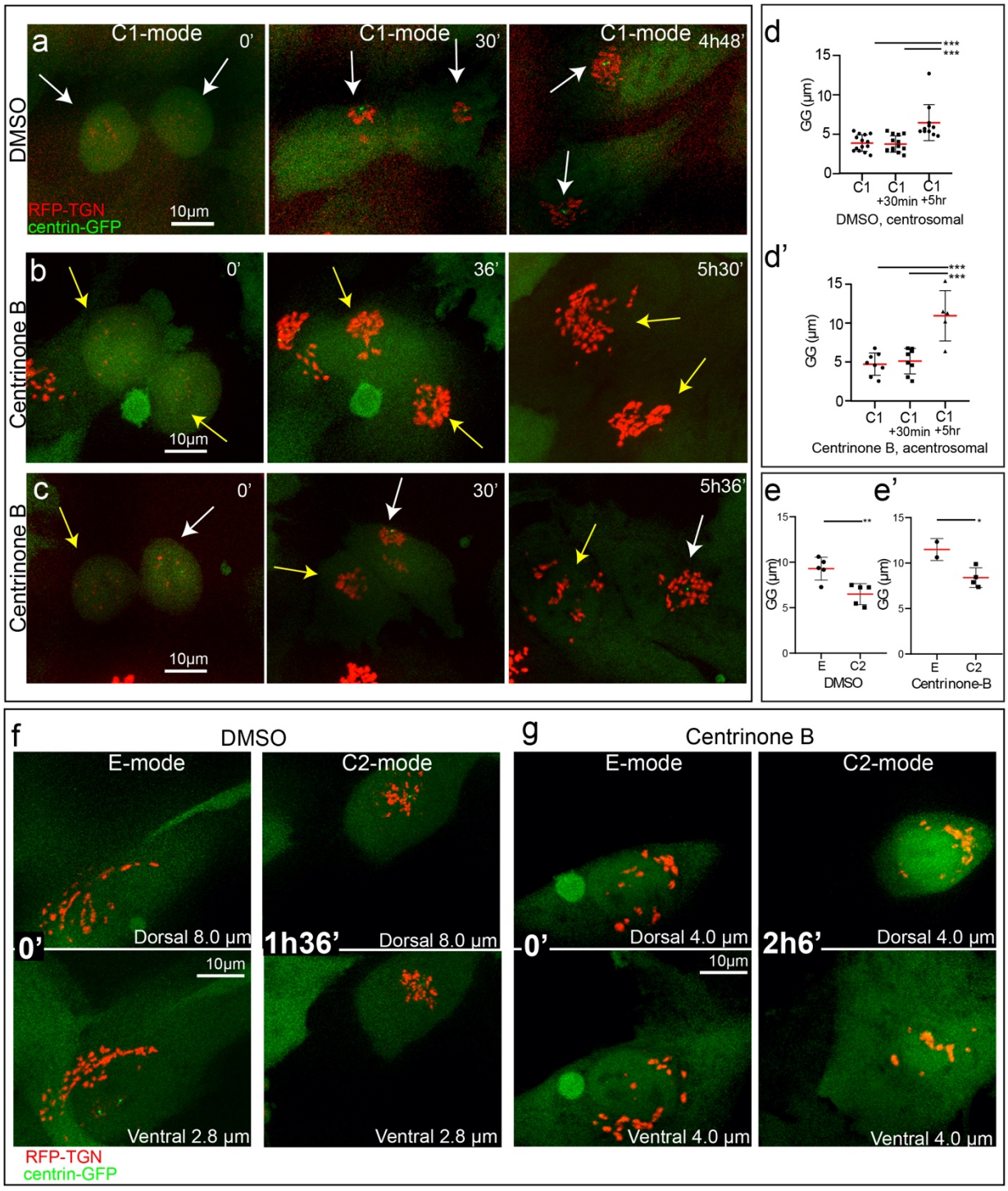

(a-c) Frames from time-lapse imaging sequences of dividing RPE1 cells stably expressing Golgi (RFP-TGN, red) and centrosome markers (centrin1-GFP, green), C1 mode progression within a 5 hour period in control cell (a) or cells pre-treated by Centrinone B for

72 hours and containing no centrosomes (b) or one centrosome (c). Daughter cells with centrosomes, white arrows. Daughter cell without centrosome, yellow arrow. Note compact Golgi configuration in all daughter cells after the mitotic exit, and early E mode in acentrosomal cell at 5h. Scale 10 μm. Time, hours, minutes. (d-d') GG distance determined for control (d) and acentrosomal (d') cells at 6-12 min after mitotic exit is referred to as "C1", 30 mins and 5 hours, referred to as "C1+30mins," and "C1+5h", respectively. Based on data as in (a-c). At a later time point (5h), GG in acentrosomal cells is significantly higher than at the earlier time points (Student t-test, ***$p<0.001$). It is also significantly higher than GG at 5h time point in DMSO (Student t-test, $p<0.01$). n=11). (e-e') GG distance determined for E mode to C2 mode transition in RPE1 cells stably expressing Golgi and centrosomes. Control (DMSO, e) does not significantly differ from acentrosomal cells (Centrinone B, e'). Student t-test showed significant differences (**$p<0.01$) between E mode and C2 mode after DMSO treatment and significant difference (*$p<0.05$) between E mode and C2 mode in Centrinone B treated cells. n=3-4. Error bars, SD. Red line, mean. (f-g) Frames from time-lapse imaging sequences of dividing RPE1 cells stably expressing Golgi (RFP-TGN, red) and centrosome markers (centrin1-GFP, green), E mode to C2 mode transition within a 2 hour period in control cell (f) or cells pre-treated by Centrinone B for 72 hours and containing no centrosomes (g). Images are maximum intensity projection of dorsal or ventral part of spinning disk confocal stacks. Size of stack is indicated in each image. Scale, 10 μm. Time, hours, minutes.

Centrosomes Are Dissociated from the Golgi during Pre-Mitotic Centrosome Separation

Thus far, our data demonstrate that the Golgi has a reproducible pattern of association and dissociation from the centrosome within the cell cycle, and that transitions between the compact and spread Golgi morphologies occur in a centrosome-independent manner. This prompted us to investigate whether the Golgi influences behavior of the centrosome.

The two centrioles inherited by each cell during mitosis form a common complex in the majority of RPE1 cells (Panic et al., 2015) which often resides near the Golgi between the nucleus and the advancing edge of the cell (Ridley et al., 2003). Consistent with this notion, in fixed-cell analyses we observe short centriole-centriole (CC) mean distances in G1 (0.62 ± 0.27 μm, N = 104) and S (0.74 ± 0.51 μm, N = 151) phases. Both mean CC distance and variance of the distribution increase significantly in G2 cells (2.48 ± 3.71 μm, N = 54) and the mean further increases among prophase cells (5.14 ± 3.24 μm, N = 47). These changes suggest that the common complex comprising two mature centrioles breaks down some time in G2 and the released centrioles move away from each other. This behavior is expected as the two centrosomes are consistently found on the opposite sides of the nucleus either on its dorsal and ventral surfaces (~75% of cells, Magidson et al., 2011) or near the opposite edges near the nuclear equator (~25% of cells, Magidson et al., 2011). To detail the pattern of centrosome separation and correlate it with the behavior of Golgi we followed behavior of centrioles labeled via constitutive expression of centrin1-GFP (Figure 5a, Movie 13). Analysis of 13 cells suggests that the duplicated centrioles (diplosomes) begin to separate ~1 hr prior to NEB. The diplosomes initially move away from each other along the nuclear envelope on the same side of the nucleus. In ten cells, upon reaching the opposite edges of the nucleus, one diplosome reverses its direction and moves back towards its original position while the second diplosome moves over the edge and towards the center of the nucleus but on its opposite surface (Figure 5a, Movie 13). As a result of this complex pattern, CC transiently increases and then decreases as the centrosomes settle near the nuclear center on the ventral and dorsal surfaces. In the remaining 3 cells, upon the initial separation the centrosomes remain at the opposite nuclear edges until NEB (our unpublished observations). Germane in these observations is that separation of diplosomes from the common complex occurs late in G2 when, as described above, the Golgi is already dissociated from the centrosome.

These observations are consistent with a concurrent recording of Golgi and centrosome behaviors within the same cell (Figure 5c-d, Movies 14 and 15). In all 27 recorded movie sequences, the centrosomes were released from the common complex and started moving apart (CC distance > 2.5μm) significantly later than dissociation of the centrosome from the Golgi (295 ± 179 min; min=42 min; max=648min). A sharp increase in CC distance (gray arrows in Figure 5d-d") consistently occurs after the Golgi-centrosome dissociation (GC increase, red arrows in Figure 5d-d''). Consistently, at the time of the centrosome separation, Golgi has normally already acquired E mode configuration around the nucleus (high GG levels, blue arrows in Figure 5d-d'). Furthermore, the CC distance increase occurs prior to a sharp decline in GC and GG, indicative of C2 mode Golgi compaction around the centrosome (purple arrow in Figure 5d-d').

We conclude from these data that centrosome separation occurs within the period between the centrosome-Golgi dissociation and initiation of Golgi compaction. This is also the period when no correlation is observed between the Golgi-centrosome association and Golgi positioning, thus these two organelles are independent of each other. Together with the previous finding that blocking Golgi fragmentation inhibits the separation of mitotic spindle poles (Guizzunti & Seemann, 2016), our data suggest a possibility that dissociation of the Golgi from the centrosome in E mode allows for the subsequent centrosome separation process.

Figure 5. Centrosome separation occurs in E mode, after dissociation from the Golgi.

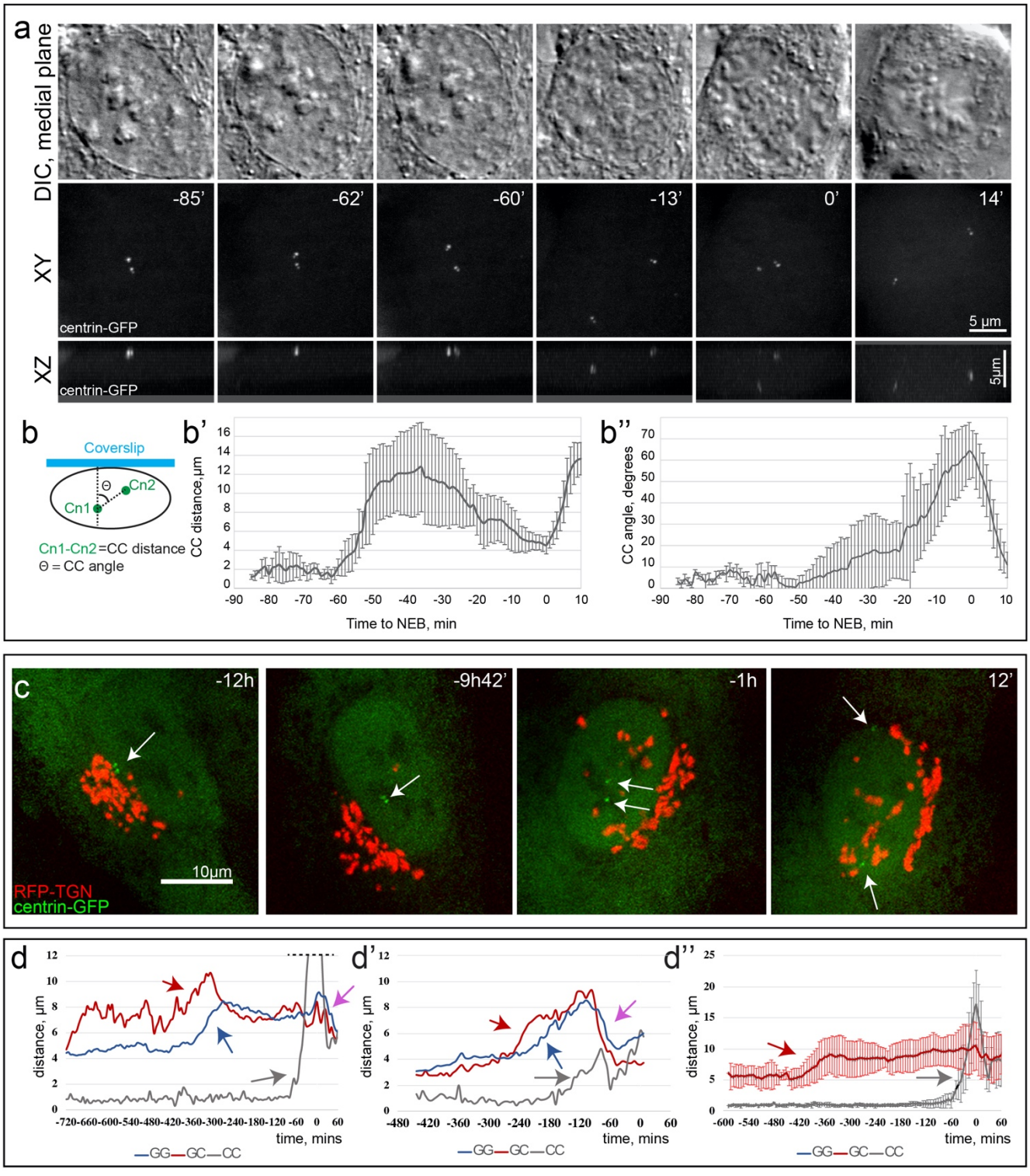

(a) Frames from multi-mode DIC (upper row) and wide-field epifluorescence 3D time-lapse recordings. GFP-centrin is shown as maximum intensity projections (middle row, XY view; lower row, XZ view). Arrows indicate centrosomes. Scale 5 μm. Time point "0" indicates NEB. Time, minutes. (b-b") Quantification of centrosome positioning in data like in (a). (b) Schematic of centrosome-centrosome (CC) distance and angle quantification. (b') Dynamics of CC distance over time. (b'') Dynamics of CC angle over time. n=13. Error bars, SD. (c) Frames from a time-lapse imaging sequence of RPE1 cells stably expressing Golgi (RFP-TGN, red) and centrosome markers (centrin1-GFP, green) during E mode progression. White arrows indicate centrosome position. Scale 10 μm. Time points correspond to values approaching "0" which indicates the maximal CC. Time, hours, minutes. Maximum intensity projection of entire spinning disk confocal stacks. (d-d') GG (blue line), GC (red line), and CC (grey line) distance profile for representative cells. Grey arrows indicate the CC distance increases after increase of GG (blue arrows) and GC (red arrows), but prior to GG/GC decreases (purple arrows) indicating C2 mode. Top of graph in 5d was cut to highlight changes in GG/GC/CC distances. Time point "0" indicates the maximal CC. Time, minutes. (d") Averaged GC (red) and CC (gray) profiles over time. Sequences aligned by the maximum CC (time point "0"). Note that GC (red arrow) increases significantly earlier than CC (grey arrow). n=11. Error bars, SD. Time, minutes.

Compact Golgi Mode Is Associated with Highest Cell Migration Speeds

The highly reproducible pattern of the Golgi morphological reorganization suggests that the process is functionally significant although the exact role of each configuration is not immediately apparent. We reasoned that one consequence of a highly compact Golgi in a motile cell is that a cell acquires a high degree of polarity due to a narrow radial distribution of the Golgi. This prompted us to assess changes in the radial distribution of Golgi with respect to the nucleus

(Figure S3) as a cell progresses through interphase (Figure 6a,b, Movie 16). When the Golgi is in C1 mode, radial histograms centered on the center of the nucleus display a single narrow peak expected for highly polarized cells (Figure 6b, time 0). This trend was typical for the overall G1 cell population (Figure 6c). As the cell progresses through the cell cycle, this peak becomes wider as the Golgi gradually spreads equatorially (Figure 6b,c). This indicates a gradual decrease in polarity throughout interphase and prophase.

Because Golgi integrity and positioning is an important factor in motile cell polarity (Farhan & Hsu, 2016) and Golgi scattering impairs directional cell migration (Miller et al., 2009; Prigozhina & Waterman-Storer, 2004; Yadav et al., 2009) we correlate radial distribution of the Golgi with the velocity of cell migration in motile cells over the course of interphase. We observe that cells with compact Golgi move more efficiently and cover longer distances (Figure 6d-e', Movies 17 and 18) than cells with Golgi positioned more equatorially. Further, we observe a clear correlation between the value of PER that characterizes equatorial spread of the Golgi and the main parameters of migration (Figure 6). Specifically, cells with PER values lower than 25% (typical for cells that exited mitosis recently) display a higher velocity (Figure 6f), higher directional persistence (Figure 6g), and longer displacements (Figure 6h). Thus, Golgi compaction appears to define the extent of motile cell polarization and influence cell motility in a cell-cycle-dependent manner

Figure 6. C1 Golgi compaction correlates with high cell migration speeds.

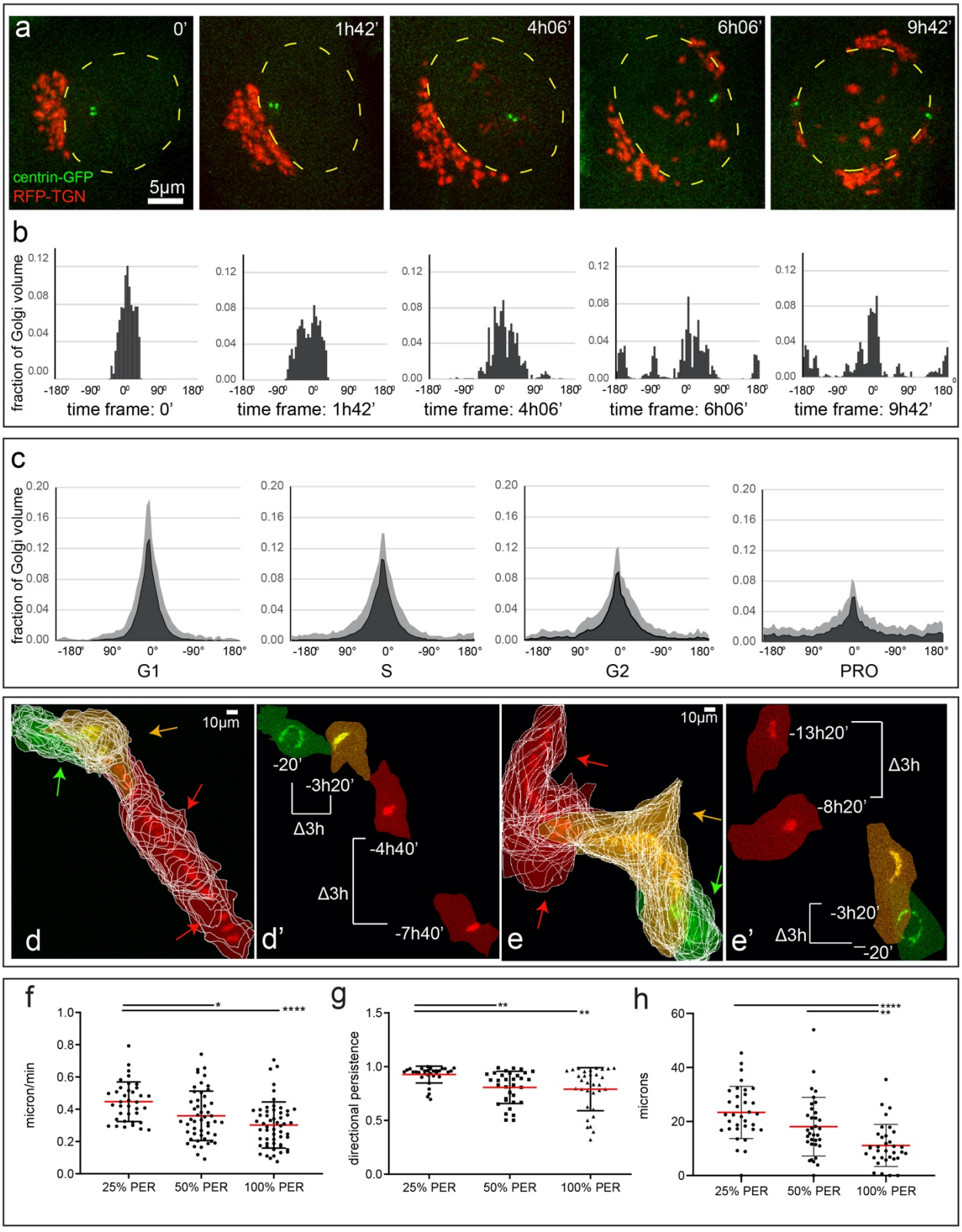

(a) Frames from time-lapse imaging sequences of an RPE1 cell stably expressing Golgi (RFP-TGN, red) and centrosome markers (centrin1-GFP, green) during E mode progression. Yellow dotted lines indicate nucleus outline. Maximum intensity projections of laser scanning confocal stacks. Scale 5 μm. (b) Histograms of radial Golgi distribution in the cell shown in (a), corresponding to each timepoint above. Fraction of Golgi volume in 5-degree radial sectors are plotted. Angle 0 indicates the bin with the largest number of Golgi voxels. c) Mean histograms of radial Golgi distribution per cell cycle stage for entire fixed cell population (as used in Figure 1b-d). SD is shown in light gray. (d-e') Overlaid frames from time-lapse epifluorescence imaging sequences of RPE1 cells stably expressing Golgi marker (RFP-TGN). Images are pseudo-color-coded according to Golgi configuration modes: compact Golgi (PER <25%, red), early E mode (PER=25-50%, yellow), and advanced E mode (PER>50%, green). (d,e) Frames with 10 minute intervals are overlaid. Cell outlines are shown in white. Note large displacements between cells with compact Golgi (red arrows), and smaller displacements between cells with early (yellow arrows) and advanced (green arrows) E mode. (d', e') Selected frames with 3-hour intervals between cells in C1 (red) and E mode (yellow, green). Note that displacement (△3h) for C1 mode is larger than for E mode. (f-h) Cell migration parameters according to the Golgi configuration (PER). (f) Speed measured in microns per minute. (g) Directional persistence (0-1; 0 indicating random cell trajectory, 1 indicating straight trajectory). (h) Displacement measured in microns over one hour. One-way ANOVA with Tukey's multiple comparison was used to determine differences (*$p<0.05$). Scale 10 μm. Time, hours, minutes. Error bars, SD. Red line, mean.

Discussion

This study highlights the dynamicity of the Golgi complex's morphology and its association with the centrosome throughout the cell cycle substages. Several key findings can be taken from this work. First, the Golgi complex transitions between periods of high compactness around the centrosome and perinuclear extension away from the centrosome (Figure 7a). These configuration modes are highly correlative with the cell cycle substages. Compact mode 1 (C1 mode) corresponds to cells newly exited from mitosis, thus G1 cells (Figure 7a, left). The equatorial mode (E mode) is characterized by dissociation of the centrosome from the Golgi and proximity of the Golgi and the nuclear envelope. The degree of Golgi extension around the nucleus increases during S-phase and culminates with the Golgi complex stretched around the perimeter of the nucleus at late G2 or early prophase (Figure 7a, center). Next, there is a quick flip to a second state of high Golgi compactness close to the centrosomes, usually directly prior to the NEB (Figure 7a, right). Our data indicate that there is a regulated switch from the compact to extended Golgi configuration in S-phase and an opposing switch from extended to compact configuration in prophase. It is reasonable to imply that the mechanism driving Golgi compactness remains activated throughout mitosis to keep remaining Golgi elements proximal to the spindle poles during division (Wei & Seemann, 2009), and driving compaction of emerging Golgi in daughter cells.

In addition to describing the dynamic changes in interphase cells, our data show the contribution of microtubules and centrosomes in cells adopting these described Golgi membrane configurations. In accordance with all prior research, we show that Golgi morphology and rearrangement absolutely relies on MTs and MT-dependent transport (Figure 7b). Because all Golgi modes persist in acentrosomal cells, it is likely that non-

centrosomal Golgi-derived MTs are sufficient to support Golgi rearrangements, as we have previously demonstrated for Golgi complex assembly (Miller et al., 2009; Vinogradova et al., 2012). The role of the centrosomes is more complex. Prior research has shown the Golgi complex and the centrosomes are closely associated in interphase (Rios & Bornens, 2003; Sütterlin & Colanzi, 2010). This connection is initiated and maintained by the MT motor dynein which positions ER-to-Golgi carriers and Golgi membranes at the concentration of MT minus ends around the centrosome (Lippincott-Schwartz et al., 1989; Miller et al., 2009; Presley et al., 1997; Yadav et al., 2012a). Additionally, linker proteins like AKAP450 (Hurtado et al., 2011) or GM130 (Tormanen et al., 2019) were implicated in directly connecting the two organelles. Importance of interphase Golgi-centrosome association for cell polarity, migration, ciliogenesis, and other functions was suggested in a number of studies (Hurtado et al., 2011) but challenged by others (Tormanen et al., 2019). Another solid body of studies indicates that fragmented Golgi elements are concentrated around the centrosome in mitosis to support equal partitioning of Golgi membranes into daughter cells (Seemann et al., 2002). This concept was also challenged by the finding that Golgi can reemerge from the ER upon mitotic exit, thus equal partitioning might not be absolutely necessary (Lippincott-Schwartz et al., 1989; Shima et al., 1997).

Our study is unique because it determines a cell cycle time frame when Golgi-centrosome association does not apply, highlighting the necessity of controlling this bond and indicating that it is indeed an important cellular function, and not a coincidence. Moreover, we find that the centrosome separation prior to mitosis occurs within this time frame (Figure 7c, center). Interestingly, prior studies have found that artificial blocking of Golgi dynamics results in monopolar mitotic spindle assembly (known to arise from a lack of centrosome separation), interpreted as a necessity for Golgi disassembly in

mitosis (Guizzunti & Seemann, 2016) . However, our study shows that the Golgi-centrosome bond is dissolved in interphase and re-established in prophase following centrosome separation. Combined, prior and our data indicate that it is important to dissociate the Golgi from the centrosome prior to mitosis for efficient centrosome separation and bipolar spindle assembly, while these two organelles re-associate at the mitotic entrance (C2 mode) to assure perfect Golgi partitioning (Figure 7c, right).

On the other hand, we find that Golgi compaction itself, and not only the Golgi-centrosome bond, is a cell cycle-regulated phenomenon, because in acentrosomal cells it occurs at the same stages as in control. These data suggest that the cell cycle switch that initiates Golgi configuration modes likely involves change in molecular motor activity. In particular, minus-end directed motor must prevail during G1 and late prophase, and plus-end directed motor during S-phase and G2 (Figure 7b). Such switches might involve activation or inactivation of motors of opposite polarity, or a change in one motor's activity which subsequently influences the direction of transport via the tug-of-war motor interplay (Mü et al., 2008).

Temporal activation/inactivation of Golgi compactness in interphase is likely an important functional phenomenon, because the integrity of the Golgi complex is important for polarization of motile cells and directional cell migration (Bisel et al., 2008; Prigozhina & Waterman-Storer, 2004; Ravichandran et al., 2020; Tormanen et al., 2019). Polarized orientation of the Golgi towards the motile cell front allows it to serve as a source of polarity factors (Farhan & Hsu, 2016) and front-directed MTs (Efimov et al., 2007), which deliver post-Golgi trafficking (Miller et al., 2009), mRNA (Gagnon & Mowry, 2011), and other materials to the protruding edge. Our new data indicate that Golgi configuration fine-tunes this polarity function: highly compact Golgi (C1 mode) in G1 is apparently capable of providing very focused polarity cues, while wide, equatorially

extended Golgi (E mode) is radially scattered and less efficiently supports polarity. Because Golgi configuration is driven by the cell cycle, cells in G1 consistently move the fastest and most persistently (Figure 7c, left). As interphase progresses, cells slow down and cease migration when the Golgi reaches the full E mode, in time for mitosis. These data are consistent with previous observations that G2 cells migrate slower (Bayarmagnai et al., 2019; Walmod et al., 2004). We observe that the Golgi-centrosome proximity is minimized at the time of slower migration speed (E mode), however it was shown that Golgi-centrosome link is not directly needed for migration efficiency (Tormanen et al., 2019). Thus, it is likely that Golgi morphology and not the centrosome link is important for cell-cycle-dependent migration efficiency (Figure 7c, left).

Our research also suggests C2 mode occurs prior to nuclear envelope breakdown. The phosphorylation of nuclear envelope proteins, such as NUP (Prunuske & Ullman, 2006) has been widely accepted as initiating NEB. Moreover, NEB is considered to be a concerted effort between the aforementioned mechanism and mechanical tension on the nuclear envelope (Beaudouin et al., 2002) exerted by microtubules and resulting in the tearing of the nuclear lamina. Our data show that without the centrosomes and subsequently the centrosome microtubule array, NEB is unaffected. This suggests that the microtubules nucleated at the Golgi located in direct proximity to the nucleus (late E and C2 modes) are sufficient for providing tension for a successful NEB event. Overall, our data indicate that Golgi configuration and association with the centrosome are tightly regulated within the cell cycle. Combined with the previous knowledge, our findings indicate that each Golgi configuration is associated with a specific function and is significant for cell physiology.

Figure 7. Model of Golgi-centrosome relationships throughout the cell cycle.

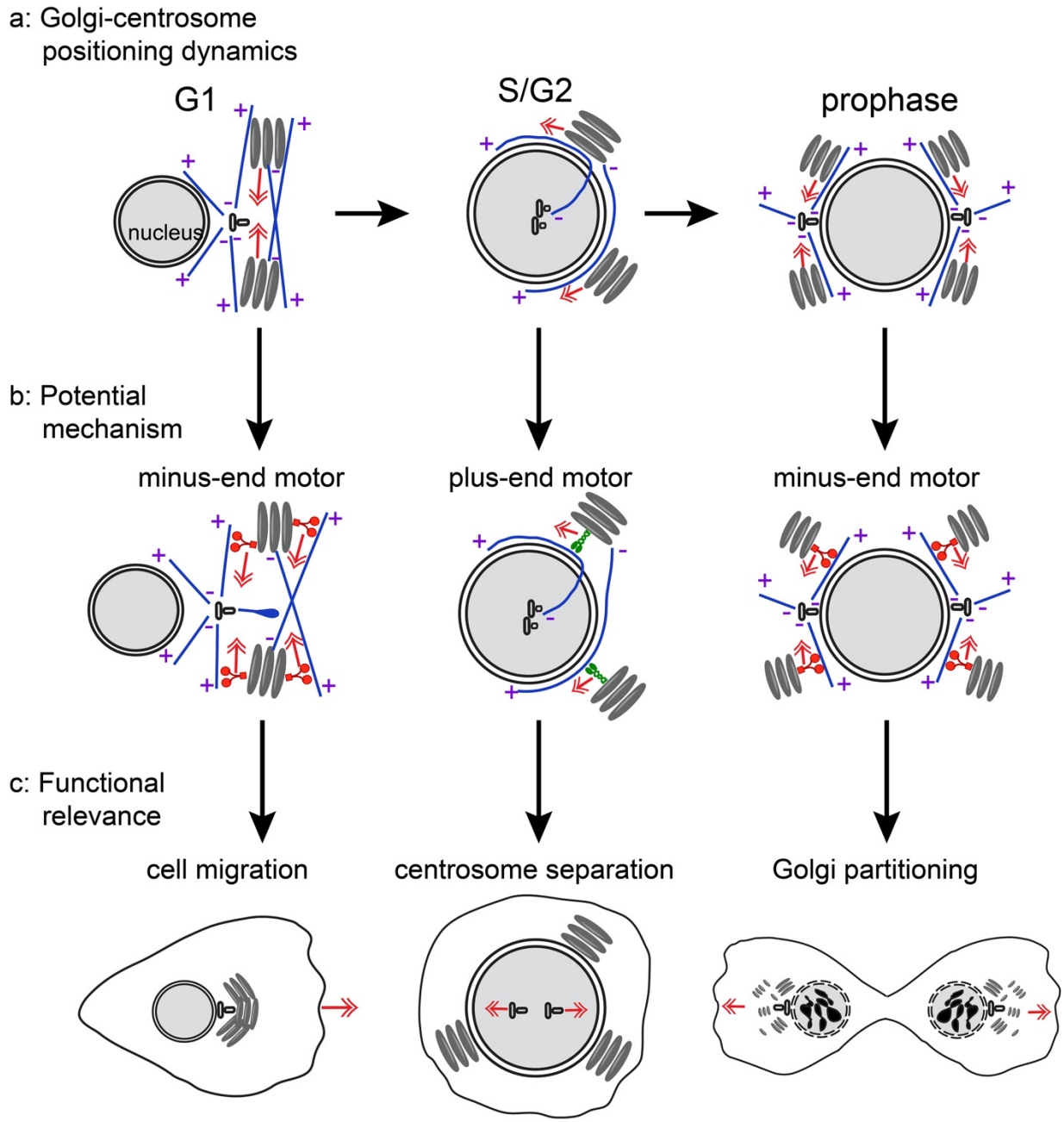

(a) Golgi and centrosome association and positioning in G1 (C1 mode, left), S/G2 (E mode, center), and prophase (C2 mode, right). Both centrosomal and Golgi-derived MTs serve as tracks for Golgi movement. (b) Proposed mechanism driving Golgi configuration in the stages

according those depicted in (a). Because the centrosomal MT aster is dispensable for the Golgi configuration, it is likely that switches in molecular motor activity are involved. Minus-end directed motor activity prevails in compact Golgi modes (b, left and right). Plus-end directed motor transport along peri-nuclear MTs prevails during E mode (b, center). (c) Cellular functions that correlate with Golgi configuration modes depicted in (a), based on our findings and the literature. Compact Golgi in G1 supports cell polarity and migration (c, left). Detachment of the centrosome from the Golgi in E mode allows for the pre-mitotic centrosome separation (c, center). Concentration of Golgi fragments at the mitotic poles support efficient Golgi partitioning during cell division (c, right).

Supplementary Materials

Figure S1. Golgi mode quantitative parameters and their correlative relationships.

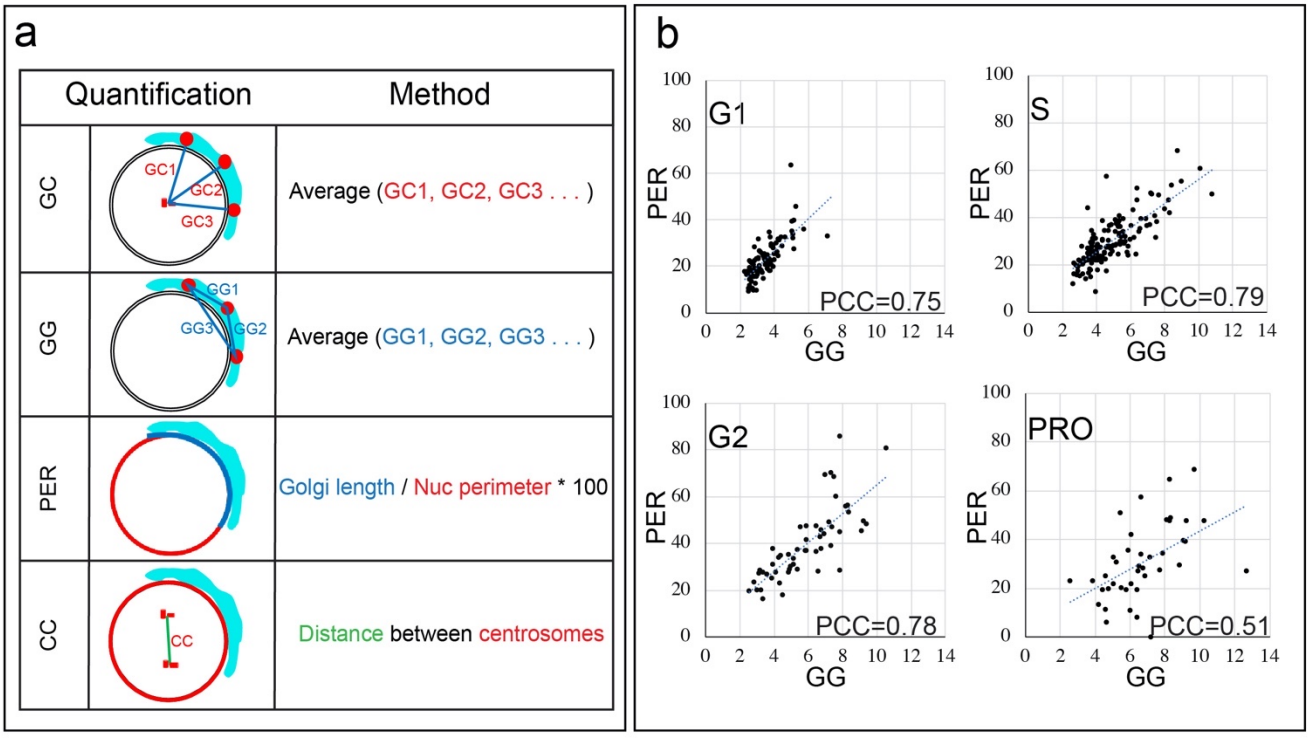

(a) Table summarizes computation of each Golgi and centrosome positioning parameter used for quantification (See Materials and Methods). (b) Correlation plots of 2D (PER) vs 3D (GG) Golgi configuration indices per cell cycle stage. High Pearson's correlation coefficient (PPC) for PER vs GG correlations indicates that they can be used interchangeably to describe the degree of Golgi-centrosome association/dissociation. n=343. The data used in (b,c) are the same as in Figure 1b-e, based on images as in Figure 1a.

Figure S2. Diversity of Golgi configuration and Golgi-centrosome association in S-phase and prophase.

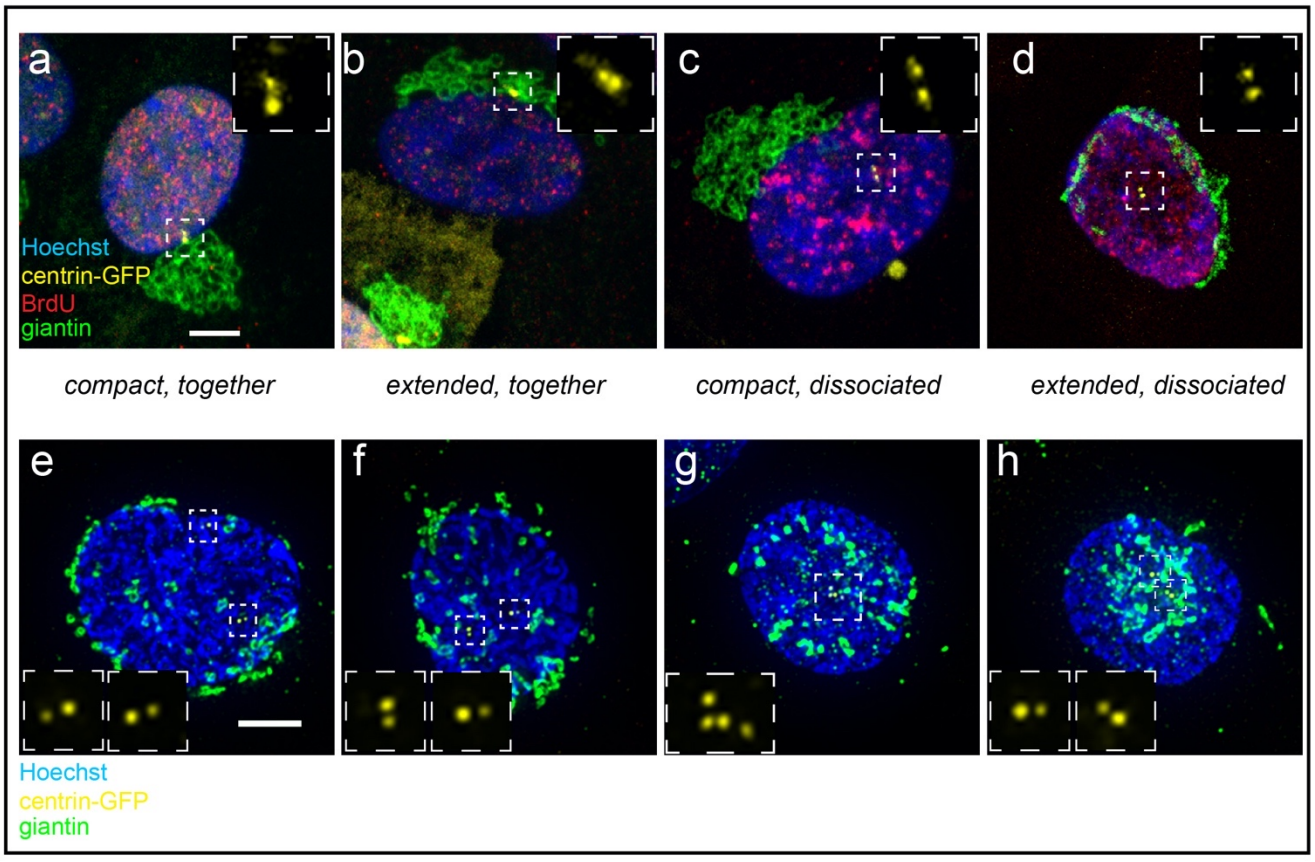

(a-d) Examples of variable Golgi and centrosome positioning in S-phase. Staining: Hoechst (blue), centrin1-GFP (yellow), BrdU (red), giantin (green). Boxed regions (centrosomes) are enlarged in

insets. Maximum intensity projections of laser scanning confocal stacks. Scale 5 µm. (e-h) Examples of variable Golgi and centrosome positioning in prophase. Staining: DAPI (blue), centrin1-GFP (yellow), giantin (green). Boxed regions (centrosomes) are enlarged in insets. Maximum intensity projections of laser scanning confocal stacks. Scale 5 µm.

Figure S3. Examples of radial Golgi distribution quantification.

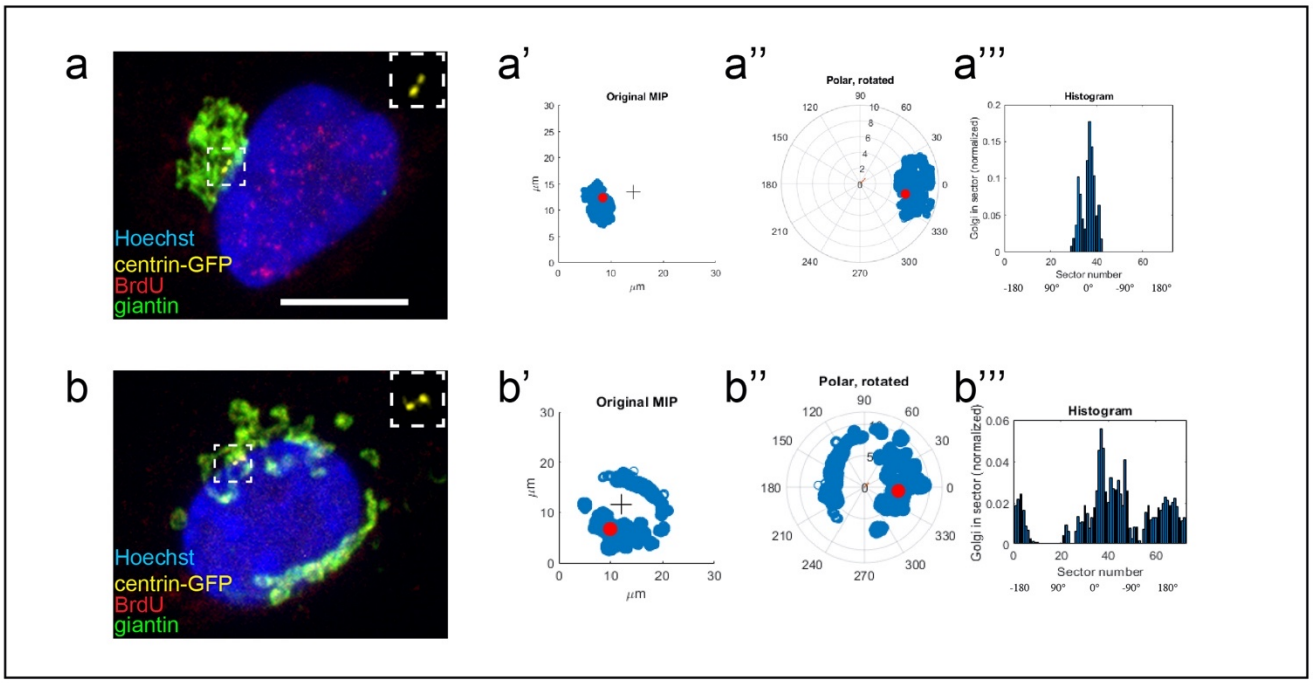

(a-a') Example of compact (high polarity) radial Golgi distribution. (b-b') Example of equatorial (low polarity) radial Golgi distribution. (a,b) Maximum intensity projections of laser scanning confocal stacks. Immunostaining: Hoechst (blue), centrin1-GFP (yellow), BrdU (red), giantin (green). Scale 10 µm. (a', b') Map of Golgi density (blue) in original 2D coordinates. Centrosome center position, red. (a'', b'') Map of Golgi density (blue) in radial 2D coordinates. Centrosome center position, red. (a''', b''') Histograms of radial Golgi distribution for individual cells.

Methods

Cell culture

Immortalized human retinal pigment epithelial cells hTert-RPE1 (CRL-4000, ATCC) were maintained in DMEM/F12 with 10% fetal bovine serum, 100 μM penicillin, and 0.1 mg/ml streptomycin at 37°C in 5% CO_2. In all live-cell experiments, cells were maintained on the microscope stage at 37°C in 5% CO_2. Cells were plated on glass coverslips or glass bottom dishes (MatTek Corporation, No. 1.5, 14mm circular) coated with 5 μg/ml fibronectin (EMD Millipore, MA) 24 hours prior to experiments.

Treatments

For MT depolymerization during live-cell imaging, cells were first treated on ice for 45 mins, then the media was replaced with warm media containing 8.3 μM nocodazole (Sigma-Aldrich, St. Louis, MO, M1404). Nocodazole was prepared at 16.6 mM in DMSO. For centrosome depletion experiments, Centrinone B (Tocris, Minneapolis, MN) was prepared at 1.1 mM in DMSO. Cells were treated with 500 nM for 72 hours before live-cell imaging or fixation.

S-Phase Determination

Bromodeoxyuridine (Fischer) was prepared at a stock solution of 10 mM in PBS. Cells were treated with 10 μM BrdU for 5 mins before fixation (see below for details). Cells were then treated with 1.5 N HCl for 40 mins required for antigen retrieval. Routine antibody staining protocol was utilized after 15 min PBS wash. Additionally, EdU (ABP Biosciences, Beltsville, MD) was also used to detect S phase cells. Cells were treated for 5 mins with 10 μM EdU before fixation (see below for details). Manufacturer protocol was followed as directed for EdU detection using iClick reaction technology.

Expression constructs

One of two RPE1 stable cell lines were used for most experiments. (1) Centrin1-GFP was introduced into RPE1 cells by lentiviral incorporation of the construct (Lončarek et al., 2010) (2) Centrin-1-GFP RPE1 cells were then transfected with RFP-TGN (gift from Enrique Rodriguez-Boulan, (Deora et al., 2007) via Amaxa (Lonza, Program I-013) then selected with G418 for at least two weeks before cell sorting. ES-FUCCI (gift from Pierre Neveu (Addgene plasmid # 62451), mCherry-NLS (gift from Dylan Burnette), and membrane-anchored GFP-gtn, (gift from Adam Lindsted (Yadav et al., 2012a)) were transfected into RPE1 cells using Amaxa or Fugene (Promega, Madison, WI) according to manufacturer's protocols.

Immunostaining

For Golgi identification, mouse monoclonal antibody against GM130 (BD Transduction Laboratories, San Jose, CA) or rabbit polyclonal antibody against giantin (Abcam, Cambridge, MA) was used. MTs were stained with anti–α-tubulin rabbit polyclonal antibody (Abcam, Cambridge, MA). S-phase cells were detected by α-mouse BrDU (G3G4 (anti-BrdU) was deposited to the DSHB by Kaufman, S.J. (DSHB Hybridoma Product G3G4 (anti-BrdU)) or iClick EdU Andy Fluour 555 Imaging kit (ABP Biosciences, Beltsville, MD)). For MT and Golgi staining, cells were fixed (15 min at room temperature) in 4% paraformaldehyde, 0.025% glutaraldehyde, and 0.3% Triton in cytoskeleton buffer (10 mM 2-(N-morpholino)ethanesulfonic acid, 150 mM NaCl, 5 mM ethylene glycol tetraacetic acid, 5 mM glucose, and 5 mM MgCl2, pH 6.1). Alexa 647–conjugated highly cross-absorbed goat anti-rabbit immunoglobulin G (IgG) antibodies and Alexa 568–conjugated goat anti-mouse IgG antibodies (Molecular Probes, Invitrogen, Eugene, OR) were used as secondary antibodies. Coverslips were mounted in Vectashield Mounting Medium (Vector Labs, Burlingame, CA). DNA was detected using either DAPI (Fisher) or Hoechst 33457 (Fisher).

Image acquisition of live and fixed samples

2-color 3D live-cell imaging was performed using spinning disk Yokogawa CSU-X1 confocal based on a Nikon Eclipse Ti-E inverted microscope with an SR Apo TIRF 100x NA1.49 oil lens and either Andor DU-897 X-11240 or Photometrics Prime 95B cameras. Z-stacks with planes separated by 0.5 um over the whole cell volume were captured every 20 seconds (Figures 2h and 3f-h) or 6 mins (all other figures).

Centriole behavior (Figure 4a) was visualized in multi-mode (DIC and wide-field epifluorescence) 3D time-lapse recordings on a Nikon TE20002E microscope equipped with 100x 1.45NA PlanApo lens. Seventeen z-planes separated by 0.5 um were captured every 5 mins for both modalities. Images were recorded on an Andor iXon DU897 camera at 107 nm/pixel magnification. The microscope was controlled by IPLab software (Scanalytics). 3D movements of mother centrioles were tracked using Imaris software (Bitplane, Concord, MA).

3D laser-scanning confocal imaging of fixed cells was performed using Nikon A1r based on a Ti-E inverted microscope with SR Apo TIRF 100x NA1.49 oil lens run by NIS Elements C software (most data), or a Leica TCS SP5 microscope with an HCX PL APO 100x oil lens, NA 1.47 (Figures 3E-E'' only).

Cell migration recording (Figure 6d,e) was performed as semi-simultaneous wide-field fluorescent and DIC imaging (10 mins/frame) at an inverted Nikon TE2000E microscope with a Perfect Focus System using a 20x lens and a CoolSnap HQ CCD camera (Photometrics) driven by IPLab software (Scanalytics).

Quantitative analyses

Centrosome Distance Parameters.

Centrosome position was determined using automatic detection of the intensity maximum of the centrioles using Imaris program (Bitplane). Both centrioles were tracked in G1 cells, and

mother centriols in S and G2 cells. For live image sequences, manual tracking implementing the same algorithm was used. Centrosome-to-centrosome distance (CC), 3D, was calculated by measuring the distance of centrosome foci in a single cell over time. Centrosome-Golgi separation is defined as the centrosomes moving greater than 3 μm away from the Golgi mass. Centrosome-centrosome separation is defined as duplicated centrosomes moving greater than 2.5 μm away from each other.

Golgi and Centrosome Positioning Parameters (Suppl. Figure S1a):

For Golgi segmentation, the level of background was determined based on intensity histograms of maximum intensity projections, where the background intensities show as a gaussian distribution in the low part of the histogram. The threshold at 5% intensity above the background was thereafter implemented to full 3D image stacks. Importantly, the background was identified individually for each live imaging sequence to accommodate variability of the Golgi marker expression level. For fixed images, the background was identified per experimental repeat to account for variability of immunostaining intensity.

For Golgi to centrosome distance (GC), the distance from each voxel within segmented volume of the Golgi to both centrosomes was determined, and the mean distance to the nearest centrosome was calculated to describe Golgi association with the proximal centrosome. The spread of Golgi (GG) was calculated as the mean of pairwise distances for all voxels within segmented volume of the Golgi. Both parameters were calculated in Matlab (MathWorks, Natick, MA). Percentage of Equatorial Redistribution (PER), 2D, was determined by manually measuring the nuclear perimeter and the length of Golgi less than 2μm away from nucleus in a maximum intensity projection of each cell. Calculating the ratio of the two measures produces PER values.

Radial distribution of Golgi

Radial distribution of Golgi was assessed by the number of voxels within 5-degree segments in 2D polar coordinates with the origin coinciding with the center of the nucleus (Suppl. Figure S3). Angle 0 was assigned to the center of bin with the largest number of segmented voxels, i.e., the largest volume of Golgi. Radial histograms were calculated in Matlab (MathWorks, Natick, MA).

Nuclear Envelope Breakdown (NEB)

To determine point of NEB, maximum intensity projections of the mCherry-NLS channel were registered with the ImageJ StackReg plugin, using the translation function. An ROI was drawn in the cytoplasm of each cell and the mean intensity of the selection was measured and plotted overtime. Intensity curves of 8 cells were normalized and aligned based on a value of 1, indicating the time point where the NLS signal was the highest in the cytoplasm. We consider this the point of NEB. Golgi compaction in Golgi-mode C2 was determined independently of NLS leakage. The Golgi channel was observed for the changes of the Golgi configuration. The timepoint where there was detection of Golgi particles moving toward spindle poles is designated as the start of C2. The start of C2 and the peak of NLS intensity of several cells were then plotted on one graph to determine any correlation of the timing of the two events.

Cell Migration Speed, Displacement, Directional Persistence

RPE1 cells expressing RFP-TGN were imaged using spinning disk microscopy. Both the Golgi fluorescence and DIC images were recorded. DIC was used to track the cell trajectory every 10 mins using the MTrackJ plugin in ImageJ. The center of the nucleus was used as a reference point for tracking. All movies used for analysis were 60 mins long. To determine changes in cell migration parameters (speed, displacement, directional persistence) output from this tracking macro was utilized. Cells were grouped into three groups, based on each cell's PER. "<25% PER"

includes cells that were newly divided within the time lapse of the movie, with PER less than 25%. “25-50% PER” includes cells with PER between 25% and 50%. “>50% PER” included cells with PER greater than 50% that were also shown to enter mitosis within the time lapse of the movie. For each cell track, displacement was measured as the distance from start (D2S). Directional persistence was calculated as the maximum distance from the start of the track (D2S) divided by the length of the track (Len). Values approaching 1 indicate a unidirectional track.

Cell cycle analysis

BrdU (EdU) was added to culture medium of non-synchronized population of Centrin1-GFP-expressing RPE1 cells. After a five-minute BrdU (EdU) incorporation, cells were fixed and processed for immunostaining to highlight Golgi, chromatin (Hoechst) and BrdU (EdU) incorporation. BrdU (EdU)-positive cells were considered S-phase cells. Cells with condensed chromosomes and intact nucleus were considered prophase. Cells with condensed chromosomes and no intact nucleus were considered in post-NEB mitosis. Cells with two centrioles were considered G1. Cells with four centrioles and no BrdU (EdU) incorporation were considered G2. Cells where centrioles number could not be identified and no BrdU (EdU) incorporation were excluded from the analysis.

Statistical Analysis

All quantitative data were collected from experiments performed in triplicate or more, unless mentioned in the figure legends. Data sets were analyzed using a one-way ANOVA *F*-test, Tukey’s multiple comparison test, and/or Student’s *t* test, as described in the figure legends.

Image Processing

Image analysis was performed using ImageJ, Matlab, and Imaris. 3D image reconstruction was made using Imaris. For all fluorescence images presented here, adjustments were made to brightness, contrast, and gamma settings to make small structures visible.

Acknowledgements

We thank Hamida Ahmed and Brian S. Domin for technical help. The authors also thank Dr. Anna AWM Sanders for suggestions and critical reading of the manuscript.

This work was supported by the National Institutes of Health (NIH) grants R35-GM127098 (to I.K.), R01-DK106228 (to I.K.), and R35-GM130298 (to A.K.). K.B.F. was supported by an NIH training grant R25-GM062459 “Initiative for Maximize Student Diversity” (Sealy, PI). We utilized the Vanderbilt Cell Imaging Shared Resource (funded by NIH grants CA68485, DK20593, DK58404, DK59637, EY08126, NIH SEI10, 1sS10, 1S10OD018075, and S10OD012324) and the Flow Cytometry Shared Resource supported by the Vanderbilt Ingram Cancer Center (P30 CA68485) and the Vanderbilt Diabetes Research and Training Center (funded by NIH grant DK020593).

Author Contributions

K.F. performed majority of the experiments, analyzed the data, and wrote the manuscript. F.R. performed and analyzed experiments on centrosome tracing. M.F. made preliminary observations and performed experiments on microtubule organization. X.Z. developed quantitative analysis approaches. L.G. performed cell migration experiments. A.K. designed parts of the experimental strategy and quantitative analysis approaches, analyzed data, and edited the manuscript. I.K. conceived the project, designed the experimental strategy, performed experiments, and wrote the manuscript. All authors provided intellectual input, vetted, and approved the final manuscript.

CHAPTER III

Conclusions and Future Directions

Conclusions

The Golgi complex is a highly dynamic membrane-bound organelle with diverse roles throughout the cell. While it is most classically associated with its role in the secretory pathway where it serves as a hub for the processing and trafficking of newly synthesized proteins, the Golgi complex has been implicated in other vital cellular processes. It has long been accepted that the Golgi complex, usually described as localized near the nucleus and tightly associated with the centrosome, is held together by microtubules (Thyberg & Moskalewski, 1999). Additionally, while seminal studies show microtubules are able to grow from Golgi fragments (Chabin-Brion et al., 2001), the Kaverina lab was the first to intimately describe the process of Golgi derived microtubule (GDMT) nucleation (Efimov et al., 2007). Collectively, our studies implicate molecular players involved in GDMT formation and stability, describe GDMT dependent post-mitotic Golgi reformation, and detail GDMT roles in cell polarity and migration (Efimov et al., 2007; Miller et al., 2009; Vinogradova et al., 2012). We also have determined the oscillations of GDMT levels throughout each substage of the entire cell cycle (Maia et al., 2013). Altogether, others and our data clearly show that the intimacy of the Golgi-microtubule and Golgi-centrosome relationship deserves a deep understanding.

The present thesis work inspects the Golgi complex in the context of dynamic changes in overall Golgi morphology in specific cell cycle substages. Extensive work has been completed to study this type of Golgi dynamics in mitosis, namely, to dissect the process of Golgi fragmentation in late G2. Numerous studies have contributed to the current model whereby the classically

shaped Golgi ribbon is stepwise fragmented from a continuous interconnected Golgi ribbon, to unlinked Golgi stacks, to unstacked Golgi cisternae, and finally to vesiculated Golgi pieces throughout the cytoplasm, often concentrated at the spindle poles. According to this large body of data, a high level of fragmentation must take place, as failure to do so causes a block in mitotic entry, a concept that has been described as “the Golgi mitotic checkpoint” (reviewed in Corda et al., 2012). Additionally, it is suggested that Golgi fragmentation is not solely a means to provide small vesicular fragments for mitotic entry, but a necessity to relinquish the Golgi-centrosome bond, which thus allows the cell passage through the spindle assembly checkpoint (Guizzunti & Seemann, 2016). This concept is in alignment with the present data in that the dissociation of the Golgi and the centrosome consistently occurs in interphase but we take this concept to the next level in providing sequential steps of (1) Golgi-centrosome separation (2) advanced equatorial Golgi redistribution around the nucleus, (3) centrosome-centrosome separation, (4) re-compaction of Golgi fragments around separated separation, and (5) dissemination of Golgi vesicles at mitosis.

My thesis work is impactful as we have provided details of Golgi morphology dynamics in interphase, as previous studies were lacking at this cell cycle. The body of work provided in Chapter II confidently presents a first step in better understanding the transitions between compact and equatorial Golgi configurations by direct live cell visualization and quantitative analysis of these temporal switches. Importantly, we find that the microtubule cytoskeleton, specifically a non-centrosomal microtubule array, is necessary to facilitate these changes. Given this clue, we can begin to test hypotheses whereby the Golgi derived microtubule array provides tracks for Golgi shape changes. Additionally, we can screen GDMT associated proteins, molecular motors, and cell cycle specific signaling molecules to determine what cue incites these dynamic switches between C- and E-modes. We also specifically highlight the changes in migratory capacity of cells in compact versus equatorial modes

Future Directions

Determine cell signaling changes in S-phase that trigger compact to equatorial transition

Our data show that in early interphase, the Golgi undergoes a change from a compact to an equatorial configuration in a normal human epithelial cell line (RPE1). While the observed compact and equatorial configuration can be observed in a human cancer cell line, (HeLa, Colanzi et al., 2007) and human endothelial cell line (HPAEC, Kaverina lab unpublished), the transitions between the two configurations have not been explored. Investigating such dynamic switches would further emphasize the relevance of cell cycle dependent Golgi morphology changes. As a next step, we will determine which signaling molecules may initiate this change in Golgi morphology. An ideal candidate would have an onset of peak activity or localization to the Golgi in S phase, where we document E mode being initiated. Additionally, we cannot rule out downregulation of a signaling molecule which would allow for the release of the highly compact Golgi form. Aurora A is one of three mitotic Aurora protein kinases family members. It is special in having roles not only in mitosis, but interphase as well (Dutertre et al., 2004; Rannou et al., 2008). Specifically, it has been implicated in the maintenance of Golgi architecture and proximity to the centrosomes, solely in interphase (Kimura et al., 2018). Depletion or inhibition of the kinase leads to premature dispersal of the Golgi and significant dissociation of close Golgi-centrosome proximity (Kimura et al., 2018). By applying similar treatments to our model system and applying the various quantitative methods, we can determine if this kinase or one of its downstream targets facilitates changes in Golgi configuration. Granted, there is a plethora of potential candidates therefore we have begun to dissect results of a high throughput kinase inhibitor screen. As a first step we have utilized low resolution live cell microscopy to observe and document which inhibitor candidates negatively impact normal Golgi morphology transitions. The next steps would be to hone in on candidates and utilize higher resolution microscopy to dissect more closely how morphology is impacted. Additionally, we would determine what cell signaling changes occur in

S-phase which trigger E-mode to C2-mode transition. It is possible that the regulated step which prompts C1 to E mode is inactivated at this time, or a separate regulation event prevails during this cell cycle event.

Determine which microtubule tracks facilitate Golgi configuration changes in interphase

Our data indicate microtubules are necessary for the Golgi complex to progress from a compact configuration (C1-mode) in G1 to an extended configuration (E-mode). However, when we deplete the centrosome and thus the centrosomal microtubules array, the transition from C1- to E-mode is not disturbed. This may indicate that non-centrosomal microtubules, such as Golgi-derived microtubules (GDMTs) are fundamental in Golgi shape in interphase. There are several tools accessible to modulate this MT array. Specifically in mammalian cell culture models, AKAP450 has been determined to be essential for GDMT nucleation (Hurtado et al., 2011; Rivero et al., 2009). This large scaffolding protein has roles both at the centrosome and Golgi to recruit nucleation factors. Therefore, in addition to a depletion approach, we will utilize a dominant negative construct which specifically blocks AKAP450 function at the Golgi membrane (Kolobova et al., 2017). We will primarily utilize live cell imaging to visualize Golgi dynamics void of GDMTs and determine quantitative parameters described in detail in Chapter II.

Post-translational modifications (PTMs) of tubulin and microtubules can alter dynamics, organization, and interactions of microtubules. Acetylation is one such PTM. Pioneering studies have shown this modification is found on newly formed Golgi microtubules (Chabin-Brion et al., 2001). This would suggest stabilization of GDMTs is due to this specific PTM. If it is true that the GDMT array is responsible for changes in Golgi configuration, we can investigate whether MT stabilization due to acetylation offers stable tracks for the localization of the Golgi around the nucleus, in E-mode. This will be primarily accomplished by blocking MT deacetylation by pharmacological inhibition of the tubulin deacetylase HDAC. Blocking HDAC will allow accumulation of acetylated MTs. Detyrosination of tubulin is another PTM that correlates with

microtubule stability which we can test by inhibiting tubulin tyrosine ligase (TTL). This condition will enrich detyrosinated microtubules. Investigation of specific tubulin PTMs is relevant because specific molecular motors prefer specific PTM decorated tracks. As such, we have another means to tackle the identity of which microtubule tracks supports Golgi morphology changes.

Determine which microtubule motor(s) facilitate Golgi configuration changes in interphase

Our data suggest the directed movement of Golgi fragments along the nucleus is based on microtubule motors. We want to dissect whether a change in the localization or activity of plus or minus end motors facilitate transitions between compact and equatorial Golgi modes. Microtubule motors recognize the inherent polarity of tracks with most motors moving towards either the plus-end or the minus-end (Welte, 2004). Given this and our data which show it is likely non-centrosomal, Golgi-derived microtubules that serve as tracks for Golgi positioning at the nucleus, we can hypothesize that a minus end directed motor predominates for C1 and C2 modes while a plus end directed motor dominates during E mode.

We can postulate that just as the Golgi complex serves as the MTOC which provides MTs for Golgi configuration dynamics; dynein or a minus end directed kinesin such as KIFC3 (Xu et al., 2002) would be highly active at G1 (for C1 mode) and prophase (for C2 mode) to concentrate fragments toward this MTOC, resulting in the compact state. On the other hand, in S phase and G2 when the Golgi conforms to E mode, this minus end motor must either re-localize away from the Golgi or have reduced activity, allowing for plus end motors to dominate and support extension of Golgi fragments away from the MTOC. In support of these hypotheses, studies show that dynein is localized at the Golgi via Golgin160 in interphase (Yadav et al., 2012b) and it becomes localized at the centrosomes at S-phase and G2 (Quintyne & Schroer, 2002). Interestingly during this time period, we detect dissociation of Golgi and the centrosome and ramping up of E mode

configuration as evidenced in high Golgi-centrosome (GC) distance and high percentage of Golgi Redistribution (PER), respectively. We predict this loss of dynein at the Golgi may allow for GDMTs and kinesin motors to predominate and carry out E mode. Additionally, early studies show membrane tubules extend away from Golgi in a plus end direction via kinesin 1 (Lippincott-Schwartz et al., 1995). We will test these hypotheses by using a siRNA library to reduce expression of all molecular motors and use live cell imaging to determine any alterations in the transition through C1, E, and C2 modes.

Determine how Golgi morphology determines cell cycle-dependent migration efficiency

As our data has shown, when the Golgi complex is equatorial and the cell is moving at its slowest migration speed, the Golgi-centrosome association is maximally distal. This could suggest that the dissociation of the two organelles leads to slower cell migration. Others have also shown that the Golgi-centrosome link is not necessarily needed for migration efficiency, as seen in unperturbed wound healing assays where Golgi-centrosome association is disrupted (Tormanen et al., 2019). Therefore, in the context of the study described in Chapter II, it is more plausible to investigate the causative effect of Golgi morphology on cell migration patterns. Does a highly compact Golgi complex promote high migration speeds because of said polarity? If it is true, this too would explain the slowing of cell speeds when the Golgi is highly equatorial around the cell, and therefore no longer polar. It would be interesting to determine any correlation between improperly compacted Golgi in S phase and G2 (where the Golgi-centrosome link is dissolved) takes on similar migration speeds of cells in the same cell cycle stage which have more advanced equatorial Golgi configurations. We hypothesize these cells will acquire fast migration speeds as determined for those G1 cells.

REFERENCES

Akhmanova, A., & Steinmetz, M. O. (2008). Tracking the ends: A dynamic protein network controls the fate of microtubule tips. In *Nature Reviews Molecular Cell Biology* (Vol. 9, Issue 4, pp. 309–322). Nature Publishing Group. https://doi.org/10.1038/nrm2369

Akhmanova, A., & Steinmetz, M. O. (2019). Microtubule minus-end regulation at a glance. In *Journal of cell science* (Vol. 132, Issue 11). NLM (Medline). https://doi.org/10.1242/jcs.227850

Alberts, B., Johnson, A., Lewis, J., Raff, M., Roberts, K., & Walter, P. (2002). *An Overview of the Cell Cycle*.

Axelrod, D., Koppel, D. E., Schlessinger, J., Elson, E., & Webb, W. W. (1976). Mobility measurement by analysis of fluorescence photobleaching recovery kinetics. *Biophysical Journal*, *16*(9), 1055–1069. https://doi.org/10.1016/S0006-3495(76)85755-4

Barr, F. A., Puype, M., Vandekerckhove, J., & Warren, G. (1997). GRASP65, a protein involved in the stacking of Golgi cisternae. *Cell*, *91*(2), 253–262. https://doi.org/10.1016/S0092-8674(00)80407-9

Bayarmagnai, B., Perrin, L., Pourfarhangi, K. E., Graña, X., Tüzel, E., & Gligorijevic, B. (2019). Invadopodia-mediated ECM degradation is enhanced in the G1 phase of the cell cycle. *Journal of Cell Science*, *132*(20). https://doi.org/10.1242/jcs.227116

Beaudouin, J. L., Gerlich, D., Daigle, N., Eils, R., & Ellenberg, J. (2002). Nuclear Envelope Breakdown Proceeds by Microtubule-Induced Tearing of the Lamina. *Cell*, *108*, 83–96.

Bettencourt-Dias, M., & Glover, D. M. (2007). Centrosome biogenesis and function: Centrosomics brings new understanding. In *Nature Reviews Molecular Cell Biology* (Vol. 8, Issue 6, pp. 451–463). Nat Rev Mol Cell Biol. https://doi.org/10.1038/nrm2180

Biggins, S., & Walczak, C. E. (2003). Captivating capture: How microtubules attach to kinetochores. In *Current Biology* (Vol. 13, Issue 11, pp. R449–R460). Cell Press.

https://doi.org/10.1016/S0960-9822(03)00369-5

Bisel, B., Wang, Y., Wei, J.-H., Xiang, Y., Tang, D., Miron-Mendoza, M., Yoshimura, S., Nakamura, N., & Seemann, J. (2008). ERK regulates Golgi and centrosome orientation towards the leading edge through GRASP65. *The Journal of Cell Biology*, *182*(5), 837–843. https://doi.org/10.1083/jcb.200805045

Brandizzi, F., & Barlowe, C. (2013). Organization of the ER-Golgi interface for membrane traffic control. In *Nature Reviews Molecular Cell Biology* (Vol. 14, Issue 6, pp. 382–392). NIH Public Access. https://doi.org/10.1038/nrm3588

Burkhardt, J. K., Echeverri, C. J., Nilsson, T., & Vallee, R. B. (1997). Overexpression of the dynamitin (p50) subunit of the dynactin complex disrupts dynein-dependent maintenance of membrane organelle distribution. *The Journal of Cell Biology*, *139*(2), 469–484.

Chabin-Brion, K., Marceiller, J., Perez, F., Settegrana, C., Drechou, A., Durand, G., & Pous, C. (2001). The Golgi Complex Is a Microtubule-organizing Organelle. *Molecular Biology of the Cell*, *12*(7), 2047–2060. https://doi.org/10.1091/mbc.12.7.2047

Colanzi, A., Hidalgo Carcedo, C., Persico, A., Cericola, C., Turacchio, G., Bonazzi, M., Luini, A., Corda, D., Acharya, U., Mallabiabarrena, A., Acharya, J., Malhotra, V., Allan, V., Thompson, H., McNiven, M., Altan-Bonnet, N., Phair, R., Polishchuk, R., Weigert, R., … Lupashin, V. (2007). The Golgi mitotic checkpoint is controlled by BARS-dependent fission of the Golgi ribbon into separate stacks in G2. *The EMBO Journal*, *26*(10), 2465–2476. https://doi.org/10.1038/sj.emboj.7601686

Colanzi, A., Suetterlin, C., & Malhotra, V. (2003). Cell-cycle-specific Golgi fragmentation: How and why? In *Current Opinion in Cell Biology* (Vol. 15, Issue 4, pp. 462–467). Elsevier Ltd. https://doi.org/10.1016/S0955-0674(03)00067-X

Corda, D., Barretta, M. L., Cervigni, R. I., & Colanzi, A. (2012). Golgi complex fragmentation in G2/M transition: An organelle-based cell-cycle checkpoint. *IUBMB Life*, *64*(8), 661–670. https://doi.org/10.1002/iub.1054

De Brabander, M., Geuens, G., Nuydens, R., Willebrords, R., Aerts, F., De Mey, J., & McIntosh, J. R. (1986). Microtubule Dynamics during the Cell Cycle: The Effects of Taxol and Nocodazole on the Microtubule System of Pt K2 Cells at Different Stages of the Mitotic Cycle. *International Review of Cytology*, *101*(C), 215–274. https://doi.org/10.1016/S0074-7696(08)60250-8

Deora, A. A., Diaz, F., Schreiner, R., & Rodriguez-Boulan, E. (2007). Efficient electroporation of DNA and protein into confluent and differentiated epithelial cells in culture. *Traffic*, *8*(10), 1304–1312. https://doi.org/10.1111/j.1600-0854.2007.00617.x

Desai, A., & Mitchison, T. J. (1997). MICROTUBULE POLYMERIZATION DYNAMICS. In *Annu. Rev. Cell Dev. Biol* (Vol. 13).

Desai, A., Verma, S., Mitchison, T. J., & Walczak, C. E. (1999). Kin I kinesins are microtubule-destabilizing enzymes. *Cell*, *96*(1), 69–78. https://doi.org/10.1016/S0092-8674(00)80960-5

Duran, J. M., Kinseth, M., Bossard, C., Rose, D. W., Polishchuk, R., Wu, C. C., Yates, J., Zimmerman, T., & Malhotra, V. (2008). The role of GRASP55 in Golgi fragmentation and entry of cells into mitosis. *Molecular Biology of the Cell*, *19*(6), 2579–2587. https://doi.org/10.1091/mbc.E07-10-0998

Dutertre, S., Cazales, M., Quaranta, M., Froment, C., Trabut, V., Dozier, C., Mirey, G., Bouché, J. P., Theis-Febvre, N., Schmitt, E., Monsarrat, B., Prigent, C., & Ducommun, B. (2004). Phosphorylation of CDC25B by Aurora-A at the centrosome contributes to the G2-M transition. *Journal of Cell Science*, *117*(12), 2523–2531. https://doi.org/10.1242/jcs.01108

Efimov, A., Kharitonov, A., Efimova, N., Loncarek, J., Miller, P. M., Andreyeva, N., Gleeson, P., Galjart, N., Maia, A. R. R., McLeod, I. X., Yates, J. R., Maiato, H., Khodjakov, A., Akhmanova, A., & Kaverina, I. (2007). Asymmetric CLASP-Dependent Nucleation of Noncentrosomal Microtubules at the trans-Golgi Network. *Developmental Cell*, *12*(6), 917–930. https://doi.org/10.1016/j.devcel.2007.04.002

Etienne-Manneville, S. (2018). Cytoplasmic Intermediate Filaments in Cell Biology. *Annual*

Review of Cell and Developmental Biology, *34*(1), 1–28. https://doi.org/10.1146/annurev-cellbio-100617-062534

Evans, L., Mitchison, T., & Kirschner, M. (1985). Influence of the centrosome on the structure of nucleated microtubules. *Journal of Cell Biology*, *100*(4), 1185 1191. https://doi.org/10.1083/jcb.100.4.1185

Farhan, H., & Hsu, V. W. (2016). Cdc42 and Cellular Polarity: Emerging Roles at the Golgi. *Trends in Cell Biology*, *26*(4), 241–248. https://doi.org/10.1016/j.tcb.2015.11.003

Farquhar, M. G., & Palade, G. E. (1981). The Golgi apparatus (complex) (1954-1981) from artifact to center stage. In *Journal of Cell Biology* (Vol. 91, Issue 3 II, pp. 77s-103s). The Rockefeller University Press. https://doi.org/10.1083/jcb.91.3.77s

Feinstein, T. N., & Linstedt, A. D. (2008a). GRASP55 regulates Golgi ribbon formation. *Molecular Biology of the Cell*, *19*(7), 2696–2707. https://doi.org/10.1091/mbc.E07-11-1200

Feinstein, T. N., & Linstedt, A. D. (2008b). GRASP55 regulates Golgi ribbon formation. *Molecular Biology of the Cell*, *19*(7), 2696–2707. https://doi.org/10.1091/mbc.E07-11-1200

Ferenz, N. P., Gable, A., & Wadsworth, P. (2010). Mitotic functions of kinesin-5. *Seminars in Cell & Developmental Biology*, *21*, 255–259. https://doi.org/10.1016/j.semcdb.2010.01.019

Fletcher, D. A., & Dyche Mullins, R. (2010). Cell mechanics and the cytoskeleton. *Nature*, *463*(28), 485–492. https://doi.org/10.1038/nature08908

Frye, K., Renda, F., Fomicheva, M., Zhu, X., Gong, L., Khodjakov, A., & Kaverina, I. (2020). Cell Cycle-Dependent Dynamics of the Golgi-Centrosome Association in Motile Cells. *Cells*, *9*(5), 1069. https://doi.org/10.3390/cells9051069

Fu, J., Hagan, I. M., & Glover, D. M. (2015). The centrosome and its duplication cycle. *Cold Spring Harbor Perspectives in Medicine*, *5*(1). https://doi.org/10.1101/cshperspect.a015800

Gagnon, J. A., & Mowry, K. L. (2011). Molecular motors: directing traffic during RNA localization. *Critical Reviews in Biochemistry and Molecular Biology*, *46*(3), 229–239. https://doi.org/10.3109/10409238.2011.572861

Goodson, H. V, & Jonasson, E. M. (2018). Microtubules and microtubule-associated proteins. *Cold Spring Harbor Perspectives in Biology*, *10*(6). https://doi.org/10.1101/cshperspect.a022608

Gourret, J.-P. (1995). MODELLING THE MITOTIC APPARATUS From the discovery of the bipolar spindle to modern concepts. In *Acta Biotheoretica* (Vol. 43, Issue 9). Kluwer Academic Publishers.

Guizzunti, G., & Seemann, J. (2016). Mitotic Golgi disassembly is required for bipolar spindle formation and mitotic progression. *Proceedings of the National Academy of Sciences*, *113*(43), E6590–E6599. https://doi.org/10.1073/PNAS.1610844113

Harada, A., Takei, Y., Kanai, Y., Tanaka, Y., Nonaka, S., & Hirokawa, N. (1998). Golgi vesiculation and lysosome dispersion in cells lacking cytoplasmic dynein. *Journal of Cell Biology*, *141*(1), 51–59. https://doi.org/10.1083/jcb.141.1.51

Helenius, J., Brouhard, G., Kalaidzidis, Y., Diez, S., & Howard, J. (2006). The depolymerizing kinesin MCAK uses lattice diffusion to rapidly target microtubule ends. *Nature*, *441*(1), 115–119. https://doi.org/10.1038/nature04736

Hidalgo Carcedo, C., Donazzi, M., Spano, S., Turacchio, G., Colanzi, A., Luini, A., & Corda, D. (2004). Mitotic Golgi partitioning is driven by the membrane-fissioning protein CtBP3/BARS. *Science*, *305*(5680), 93–96. https://doi.org/10.1126/science.1097775

Hirokawa, N., Noda, Y., Tanaka, Y., & Niwa, S. (2009). Kinesin superfamily motor proteins and intracellular transport. In *Nature Reviews Molecular Cell Biology* (Vol. 10, Issue 10, pp. 682–696). Nature Publishing Group. https://doi.org/10.1038/nrm2774

Humphrey, T., & Brooks, G. (2004). *Cell Cycle Control* (Vol. 296). Humana Press. https://doi.org/10.1385/1592598579

Hunter, A. W., Caplow, M., Coy, D. L., Hancock, W. O., Diez, S., Wordeman, L., & Howard, J. (2003). The kinesin-related protein MCAK is a microtubule depolymerase that forms an ATP-hydrolyzing complex at microtubule ends. *Molecular Cell*, *11*(2), 445–457.

https://doi.org/10.1016/S1097-2765(03)00049-2

Hurtado, L., Caballero, C., Gavilan, M. P., Cardenas, J., Bornens, M., & Rios, R. M. (2011). Disconnecting the Golgi ribbon from the centrosome prevents directional cell migration and ciliogenesis. *The Journal of Cell Biology*, *193*(5), 917–933. https://doi.org/10.1083/jcb.201011014

Huxley, H. E. (1963). Electron microscope studies on the structure of natural and synthetic protein filaments from striated muscle. *Journal of Molecular Biology*, *7*(3), 281–308. https://doi.org/10.1016/S0022-2836(63)80008-X

Jesch, S. A., Lewis, T. S., Ahn, N. G., & Linstedt, A. D. (2001). Mitotic phosphorylation of Golgi reassembly stacking protein 55 by mitogen-activated protein kinase ERK2. *Molecular Biology of the Cell*, *12*(6), 1811–1817. https://doi.org/10.1091/mbc.12.6.1811

Jesch, Stephen A., Mehta, A. J., Velliste, M., Murphy, R. F., & Linstedt, A. D. (2001). Mitotic Golgi is in a dynamic equilibrium between clustered and free vesicles independent of the ER. *Traffic*, *2*(12), 873–884. https://doi.org/10.1034/j.1600-0854.2001.21203.x

Jiang, K., Hua, S., Mohan, R., Grigoriev, I., Yau, K. W., Liu, Q., Katrukha, E. A., Altelaar, A. F. M., Heck, A. J. R., Hoogenraad, C. C., & Akhmanova, A. (2014). Microtubule Minus-End Stabilization by Polymerization-Driven CAMSAP Deposition. *Developmental Cell*, *28*(3), 295–309. https://doi.org/10.1016/j.devcel.2014.01.001

Jones, M. C., Askari, J. A., Humphries, J. D., & Humphries, M. J. (2018a). Cell adhesion is regulated by CDK1 during the cell cycle. *Journal of Cell Biology*, *217*(9), 3203–3218. https://doi.org/10.1083/jcb.201802088

Jones, M. C., Askari, J. A., Humphries, J. D., & Humphries, M. J. (2018b). Cell adhesion is regulated by CDK1 during the cell cycle. *The Journal of Cell Biology*, *217*(9), 3203–3218. https://doi.org/10.1083/jcb.201802088

Jones, M. C., Askari, J. A., Humphries, J. D., & Humphries, M. J. (2018c). Cell adhesion is regulated by CDK1 during the cell cycle. *The Journal of Cell Biology*, *217*(9), 3203–3218.

https://doi.org/10.1083/JCB.201802088

Kapitein, L. C., Peterman, E. J. G., Kwok, B. H., Kim, J. H., Kapoor, T. M., & Schmidt, C. F. (2005). The bipolar mitotic kinesin Eg5 moves on both microtubules that it crosslinks. *Nature*, *435*(7038), 114–118. https://doi.org/10.1038/nature03503

Kaverina, I., Rottner, K., & Small, J. V. (1998). Targeting, capture, and stabilization of microtubules at early focal adhesions. *Journal of Cell Biology*, *142*(1), 181–190. https://doi.org/10.1083/jcb.142.1.181

Kaverina, I., & Straube, A. (2011). Regulation of cell migration by dynamic microtubules. In *Seminars in Cell and Developmental Biology* (Vol. 22, Issue 9, pp. 968–974). Elsevier Ltd. https://doi.org/10.1016/j.semcdb.2011.09.017

Kimura, M., Takagi, S., & Nakashima, S. (2018). *Aurora A regulates the architecture of the Golgi apparatus*. https://doi.org/10.1016/j.yexcr.2018.03.024

Kleylein-Sohn, J., Westendorf, J., Le Clech, M., Habedanck, R., Stierhof, Y. D., & Nigg, E. A. (2007). Plk4-Induced Centriole Biogenesis in Human Cells. *Developmental Cell*, *13*(2), 190–202. https://doi.org/10.1016/j.devcel.2007.07.002

Kolobova, E., Roland, J. T., Lapierre, L. A., Williams, J. A., Mason, T. A., & Goldenring, J. R. (2017). The C-terminal region of A-kinase anchor protein 350 (AKAP350A) enables formation of microtubule-nucleation centers and interacts with pericentriolar proteins. *The Journal of Biological Chemistry*, jbc.M117.806018. https://doi.org/10.1074/jbc.M117.806018

Koppel, D. E., Axelrod, D., Schlessinger, J., Elson, E. L., & Webb, W. W. (1976). Dynamics of fluorescence marker concentration as a probe of mobility. *Biophysical Journal*, *16*(11), 1315–1329. https://doi.org/10.1016/S0006-3495(76)85776-1

Lippincott-Schwartz, J. (1998). Cytoskeletal proteins and Golgi dynamics. *Current Opinion in Cell Biology*, *10*(1), 52–59. https://doi.org/10.1016/S0955-0674(98)80086-0

Lippincott-Schwartz, J., Cole, N. B., Marotta, A., Conrad, P. A., & Bloom, G. S. (1995). Kinesin

is the motor for microtubule-mediated Golgi-to-ER membrane traffic. *Journal of Cell Biology*, *128*(3), 293–306. https://doi.org/10.1083/jcb.128.3.293

Lippincott-Schwartz, J., & Patterson, G. H. (2003). Development and use of fluorescent protein markers in living cells. In *Science* (Vol. 300, Issue 5616, pp. 87–91). Science. https://doi.org/10.1126/science.1082520

Lippincott-Schwartz, J., Yuan, L. C., Bonifacino, J. S., & Klausner, R. D. (1989). Rapid redistribution of Golgi proteins into the ER in cells treated with brefeldin A: Evidence for membrane cycling from Golgi to ER. *Cell*, *56*(5), 801–813. https://doi.org/10.1016/0092-8674(89)90685-5

Lončarek, J., Hergert, P., & Khodjakov, A. (2010). Centriole reduplication during prolonged interphase requires procentriole maturation governed by plk1. *Current Biology*, *20*(14), 1277–1282. https://doi.org/10.1016/j.cub.2010.05.050

Lowe, M., Rabouille, C., Nakamura, N., Watson, R., Jackman, M., Jämsä, E., Rahman, D., Pappin, D. J. C., & Warrenz, G. (1998). Cdc2 kinase directly phosphorylates the cis-Golgi matrix protein GM130 and is required for Golgi fragmentation in mitosis. *Cell*, *94*(6), 783–793. https://doi.org/10.1016/S0092-8674(00)81737-7

Lucocq, J., Berger, E. G., & Warren, G. (1989). Mitotic Golgi fragments in HeLa cells and their role in the reassembly pathway. *Journal of Cell Biology*, *109*(2), 463–474. https://doi.org/10.1083/jcb.109.2.463

Lucocq, J. M., & Warren, G. (1987). Fragmentation and partitioning of the Golgi apparatus during mitosis in HeLa cells.; Fragmentation and partitioning of the Golgi apparatus during mitosis in HeLa cells. In *The EMBO Journal* (Vol. 6, Issue 11). https://doi.org/10.1002/j.1460-2075.1987.tb02641.x

Macůrek, L., Lindqvist, A., Lim, D., Lampson, M. A., Klompmaker, R., Freire, R., Clouin, C., Taylor, S. S., Yaffe, M. B., & Medema, R. H. (2008). Polo-like kinase-1 is activated by aurora A to promote checkpoint recovery. *Nature*, *455*(7209), 119–123.

https://doi.org/10.1038/nature07185

Maia, A. R. R., Zhu, X., Miller, P., Gu, G., Maiato, H., & Kaverina, I. (2013). Modulation of Golgi-associated microtubule nucleation throughout the cell cycle. *Cytoskeleton*, *70*(1), 32–43. https://doi.org/10.1002/cm.21079

Malumbres, M. (2014). Cyclin-dependent kinases. *Genome Biology*, *15*(6), 122. https://doi.org/10.1186/gb4184

Miller, P. M., Folkmann, A. W., Maia, A. R. R., Efimova, N., Efimov, A., & Kaverina, I. (2009). Golgi-derived CLASP-dependent microtubules control Golgi organization and polarized trafficking in motile cells. *Nature Cell Biology*, *11*(9), 1069–1080. https://doi.org/10.1038/ncb1920

Minin, A. A. (1997). Dispersal of Golgi apparatus in nocodazole-treated fibroblasts is a kinesin-driven process. *Journal of Cell Science*, *110*(19).

Misteli, T., & Warren, G. (1995). Mitotic disassembly of the Golgi apparatus in vivo. *Journal of Cell Science*, *108*(7).

Mitchison, T., & Kirschner, M. (1984). Dynamic instability of microtubule growth. *Nature*, *312*(5991), 237–242. https://doi.org/10.1038/312237a0

Mü, M. J. I., Klumpp, S., & Lipowsky, R. (2008). *Tug-of-war as a cooperative mechanism for bidirectional cargo transport by molecular motors*.

Nakamura, N., Lowe, M., Levine, T. P., Rabouille, C., & Warren, G. (1997). The vesicle docking protein p115 binds GM130, a cis-Golgi matrix protein, in a mitotically regulated manner. *Cell*. https://doi.org/10.1016/S0092-8674(00)80225-1

Neuhaus, J. M., Wanger, M., Keiser, T., & Wegner, A. (1983). Treadmilling of actin. In *Journal of Muscle Research and Cell Motility* (Vol. 4, Issue 5, pp. 507–527). Kluwer Academic Publishers. https://doi.org/10.1007/BF00712112

Panic, M., Hata, S., Neuner, A., & Schiebel, E. (2015). The Centrosomal Linker and Microtubules Provide Dual Levels of Spatial Coordination of Centrosomes. *PLOS Genetics*,

11(5), e1005243. https://doi.org/10.1371/journal.pgen.1005243

Pavletich, N. P. (1999). Mechanisms of cyclin-dependent kinase regulation: Structures of Cdks, their cyclin activators, and Cip and INK4 inhibitors. *Journal of Molecular Biology*, *287*(5), 821–828. https://doi.org/10.1006/jmbi.1999.2640

Paz, J., & Lüders, J. (2017). *Microtubule-Organizing Centers: Towards a Minimal Parts List*. https://doi.org/10.1016/j.tcb.2017.10.005

Peset, I., & Vernos, I. (2008). The TACC proteins: TACC-ling microtubule dynamics and centrosome function. In *Trends in Cell Biology* (Vol. 18, Issue 8, pp. 379–388). Trends Cell Biol. https://doi.org/10.1016/j.tcb.2008.06.005

Petry, S. (2016). Mechanisms of Mitotic Spindle Assembly. *Annual Review of Biochemistry*, *85*(1), 659–683. https://doi.org/10.1146/annurev-biochem-060815-014528

Piehl, M., Tulu, U. S., Wadsworth, P., & Cassimeris, L. (2004). Centrosome maturation: Measurement of microtubule nucleation throughout the cell cycle by using GFP-tagged EB1. *Proceedings of the National Academy of Sciences of the United States of America*, *101*(6), 1584–1588. https://doi.org/10.1073/pnas.0308205100

Piel, M., Meyer, P., Khodjakov, A., Rieder, C. L., & Bornens, M. (2000). The respective contributions of the mother and daughter centrioles to centrosome activity and behavior in vertebrate cells. *Journal of Cell Biology*, *149*(2), 317–329. https://doi.org/10.1083/jcb.149.2.317

Pollard, T. D. (2016). Actin and actin-binding proteins. *Cold Spring Harbor Perspectives in Biology*, *8*(8). https://doi.org/10.1101/cshperspect.a018226

Pollard, T. D., Blanchoin, L., & Mullins, R. D. (2000). Molecular Mechanisms Controlling Actin Filament Dynamics in Nonmuscle Cells. *Annual Review of Biophysics and Biomolecular Structure*, *29*(1), 545–576. https://doi.org/10.1146/annurev.biophys.29.1.545

Pollard, T. D., & Cooper, J. A. (2009). Actin, a Central Player in Cell Shape and Movement. *Science*, *326*(5957), 1208–1212.

Presley, J. F., Cole, N. B., Schroer, T. A., Hirschberg, K., Zaal, K. J. M., & Lippincott-Schwartz, J. (1997). ER-to-Golgi transport visualized in living cells. *Nature*, *389*(6646), 81–85. https://doi.org/10.1038/38001

Prigozhina, N. L., & Waterman-Storer, C. M. (2004). Protein Kinase D-Mediated Anterograde Membrane Trafficking Is Required for Fibroblast Motility. *Current Biology*, *14*(2), 88–98. https://doi.org/10.1016/j.cub.2004.01.003

Prunuske, A. J., & Ullman, K. S. (2006). The nuclear envelope: form and reformation. *Current Opinion in Cell Biology*, *18*(1), 108–116. https://doi.org/10.1016/j.ceb.2005.12.004

Puthenveedu, M. A., Bachert, C., Puri, S., Lanni, F., & Linstedt, A. D. (2006). GM130 and GRASP65-dependent lateral cisternal fusion allows uniform Golgi-enzyme distribution. *Nature Cell Biology*, *8*(3), 238–248. https://doi.org/10.1038/ncb1366

Quintyne, N. J., & Schroer, T. A. (2002). Distinct cell cycle-dependent roles for dynactin and dynein at centrosomes. *The Journal of Cell Biology*, *159*(2), 245–254. https://doi.org/10.1083/jcb.200203089

Rannou, Y., Troadec, M. B., Petretti, C., Hans, F., Dutertre, S., Dimitrov, S., & Prigent, C. (2008). Localization of aurora A and aurora B kinases during interphase: Role of the N-terminal domain. *Cell Cycle*, *7*(19), 3012–3020. https://doi.org/10.4161/cc.7.19.6718

Ravichandran, Y., Goud, B., & Manneville, J. B. (2020). The Golgi apparatus and cell polarity: Roles of the cytoskeleton, the Golgi matrix, and Golgi membranes. In *Current Opinion in Cell Biology* (Vol. 62, pp. 104–113). Elsevier Ltd. https://doi.org/10.1016/j.ceb.2019.10.003

Reck-Peterson, S. L., Redwine, W. B., Vale, R. D., & Carter, A. P. (2018). The cytoplasmic dynein transport machinery and its many cargoes. In *Nature Reviews Molecular Cell Biology* (Vol. 19, Issue 6, pp. 382–398). Nature Publishing Group. https://doi.org/10.1038/s41580-018-0004-3

Ridley, A. J. (2015). Rho GTPase signalling in cell migration. In *Current Opinion in Cell Biology* (Vol. 36, pp. 103–112). Elsevier Ltd. https://doi.org/10.1016/j.ceb.2015.08.005

Ridley, A. J., Schwartz, M. A., Burridge, K., Firtel, R. A., Ginsberg, M. H., Borisy, G., Parsons, J. T., & Horwitz, A. R. (2003). Cell migration: integrating signals from front to back. *Science (New York, N.Y.)*, *302*(5651), 1704–1709. https://doi.org/10.1126/science.1092053

Rios, R. M. (2014). The centrosome–Golgi apparatus nexus. *Philosophical Transactions of the Royal Society of London B: Biological Sciences*, *369*(1650).

Rios, R. M., & Bornens, M. (2003). The Golgi apparatus at the cell centre. In *Current Opinion in Cell Biology* (Vol. 15, Issue 1, pp. 60–66). Elsevier Ltd. https://doi.org/10.1016/S0955-0674(02)00013-3

Ríos, R. M., Sanchís, A., Tassin, A. M., Fedriani, C. N., & Bornens, M. (2004). GMAP-210 Recruits ⁄-Tubulin Complexes to cis-Golgi Membranes and Is Required for Golgi Ribbon Formation. *Cell*, *118*, 323–335.

Rivero, S., Cardenas, J., Bornens, M., & Rios, R. M. (2009). Microtubule nucleation at the cis-side of the Golgi apparatus requires AKAP450 and GM130. *The EMBO Journal*, *28*, 1016–1028. https://doi.org/10.1038/

Robert, A., Hookway, C., & Gelfand, V. I. (2016). Intermediate filament dynamics: What we can see now and why it matters; Intermediate filament dynamics: What we can see now and why it matters. *Bioassays*, *38*, 232–243. https://doi.org/10.1002/bies.201500142

Seemann, J., Pypaert, M., Taguchi, T., Malsam, J., & Warren, G. (2002). Partitioning of the matrix fraction of the golgi apparatus during mitosis in animal cells. *Science*, *295*(5556), 848–851. https://doi.org/10.1126/science.1068064

Sengupta, P., Satpute-Krishnan, P., Seo, A. Y., Burnette, D. T., Patterson, G. H., & Lippincott-Schwartz, J. (2015). ER trapping reveals Golgi enzymes continually revisit the ER through a recycling pathway that controls Golgi organization. *Proceedings of the National Academy of Sciences of the United States of America*, *112*(49), E6752-61. https://doi.org/10.1073/pnas.1520957112

Shima, D. T., Haldar, K., Pepperkok, R., Watson, R., & Warren, G. (1997). Partitioning of the Golgi Apparatus during Mitosis in Living HeLa Cells. *The Journal of Cell Biology*, *137*(6), 1211–1228. https://doi.org/10.1083/JCB.137.6.1211

Shorter, J., & Warren, G. (2002). GOLGI ARCHITECTURE AND INHERITANCE. *Annu. Rev. Cell Dev. Biol*, *18*, 379–420. https://doi.org/10.1146/annurev.cellbio.18.030602.133733

Shorter, J., Watson, R., Giannakou, M. E., Clarke, M., Warren, G., & Barr, F. A. (1999). GRASP55, a second mammalian GRASP protein involved in the stacking of Golgi cisternae in a cell-free system. *EMBO Journal*, *18*(18), 4949–4960. https://doi.org/10.1093/emboj/18.18.4949

Sjöblom, B., Salmazo, A., & Djinović-Carugo, K. (2008). α-Actinin structure and regulation. In *Cellular and Molecular Life Sciences* (Vol. 65, Issue 17, pp. 2688–2701). Cell Mol Life Sci. https://doi.org/10.1007/s00018-008-8080-8

Sladitschek, H. L., & Neveu, P. A. (2015). MXS-Chaining: A Highly Efficient Cloning Platform for Imaging and Flow Cytometry Approaches in Mammalian Systems. *PLOS ONE*, *10*(4), e0124958. https://doi.org/10.1371/journal.pone.0124958

Slangy, A., Lane, H. A., d'Hérin, P., Harper, M., Kress, M., & Niggt, E. A. (1995). Phosphorylation by p34cdc2 regulates spindle association of human Eg5, a kinesin-related motor essential for bipolar spindle formation in vivo. *Cell*, *83*(7), 1159–1169. https://doi.org/10.1016/0092-8674(95)90142-6

Smythe, E., & Ayscough, K. R. (2006). Actin regulation in endocytosis. *Journal of Cell Science*, *119*(22), 4589–4598. https://doi.org/10.1242/jcs.03247

Sönnichsen, B., Lowe, M., Levine, T., Jämsä, E., Dirac-Svejstrup, B., & Warren, G. (1998). A role for giantin in docking COPI vesicles to Golgi membranes. *Journal of Cell Biology*, *140*(5), 1013–1021. https://doi.org/10.1083/jcb.140.5.1013

Spanò, S., Silletta, M. G., Colanzi, A., Alberti, S., Fiucci, G., Valente, C., Fusella, A., Salmona, M., Mironov, A., Luini, A., & Corda, D. (1999). Molecular cloning and functional

characterization of brefeldin A-ADP- ribosylated substrate: A novel protein involved in the maintenance of the golgi structure. *Journal of Biological Chemistry*, *274*(25), 17705–17710. https://doi.org/10.1074/jbc.274.25.17705

Splinter, D., Razafsky, D. S., Schlager, M. A., Serra-Marques, A., Grigoriev, I., Demmers, J., Keijzer, N., Jiang, K., Poser, I., Hyman, A. A., Hoogenraad, C. C., King, S. J., & Akhmanova, A. (2012). BICD2, dynactin, and LIS1 cooperate in regulating dynein recruitment to cellular structures. *Molecular Biology of the Cell*, *23*(21), 4226–4241. https://doi.org/10.1091/mbc.E12-03-0210

Sütterlin, C., & Colanzi, A. (2010). The Golgi and the centrosome: building a functional partnership. *The Journal of Cell Biology*, *188*(5), 621–628. https://doi.org/10.1083/jcb.200910001

Sütterlin, C., Hsu, P., Mallabiabarrena, A., & Malhotra, V. (2002). Fragmentation and Dispersal of the Pericentriolar Golgi Complex Is Required for Entry into Mitosis in Mammalian Cells. *Cell*, *109*(3), 359–369. https://doi.org/10.1016/S0092-8674(02)00720-1

Svitkina, T. (2018). The actin cytoskeleton and actin-based motility. *Cold Spring Harbor Perspectives in Biology*, *10*(1). https://doi.org/10.1101/cshperspect.a018267

Tang, D., & Wang, Y. (2013). Cell cycle regulation of Golgi membrane dynamics. *Trends in Cell Biology*, *23*, 296–304. https://doi.org/10.1016/j.tcb.2013.01.008

Tang, D., Yuan, H., Vielemeyer, O., Perez, F., & Wang, Y. (2012). Sequential phosphorylation of GRASP65 during mitotic Golgi disassembly. *Biology Open*, *1*(12), 1204–1214. https://doi.org/10.1242/bio.20122659

Thyberg, J., & Moskalewski, S. (1999). Role of microtubules in the organization of the Golgi complex. In *Experimental Cell Research* (Vol. 246, Issue 2, pp. 263–279). Academic Press Inc. https://doi.org/10.1006/excr.1998.4326

Tormanen, K., Ton, C., Waring, B. M., Wang, K., & Sütterlin, C. (2019). Function of Golgi-centrosome proximity in RPE-1 cells. *PLOS ONE*, *14*(4), e0215215.

https://doi.org/10.1371/journal.pone.0215215

Tsou, M. F. B., Wang, W. J., George, K. A., Uryu, K., Stearns, T., & Jallepalli, P. V. (2009). Polo Kinase and Separase Regulate the Mitotic Licensing of Centriole Duplication in Human Cells. *Developmental Cell*, *17*(3), 344–354. https://doi.org/10.1016/j.devcel.2009.07.015

Turner, J. R., & Tartakoff, A. M. (1989). The response of the Golgi complex to microtubule alterations: The roles of metabolic energy and membrane traffic in Golgi complex organization. *Journal of Cell Biology*, *109*(5), 2081–2088. https://doi.org/10.1083/jcb.109.5.2081

Vaisberg, E. A., Grissom, P. M., & McIntosh, J. R. (1996). Mammalian cells express three distinct dynein heavy chains that are localized to different cytoplasmic organelles. *Journal of Cell Biology*, *133*(4), 831–842. https://doi.org/10.1083/jcb.133.4.831

Vicente-Manzanares, M., Ma, X., Adelstein, R. S., & Horwitz, A. R. (2009). Non-muscle myosin II takes centre stage in cell adhesion and migration. In *Nature Reviews Molecular Cell Biology* (Vol. 10, Issue 11, pp. 778–790). Nature Publishing Group. https://doi.org/10.1038/nrm2786

Vinogradova, T., Paul, R., Grimaldi, A. D., Loncarek, J., Miller, P. M., Yampolsky, D., Magidson, V., Khodjakov, A., Mogilner, A., & Kaverina, I. (2012). Concerted effort of centrosomal and golgiderived microtubules is required for proper golgi complex assembly but not for maintenance. *Molecular Biology of the Cell*, *23*(5), 820–833. https://doi.org/10.1091/mbc.E11-06-0550

Walmod, P. ., Hartmann-Petersen, R., Prag, S., Lepekhin, E. ., Röpke, C., Berezin, V., & Bock, E. (2004). Cell-cycle-dependent regulation of cell motility and determination of the role of Rac1. *Experimental Cell Research*, *295*(2), 407–420. https://doi.org/10.1016/J.YEXCR.2004.01.011

Wang, G., Jiang, Q., & Zhang, C. (2014). The role of mitotic kinases in coupling the centrosome cycle with the assembly of the mitotic spindle. In *Journal of Cell Science* (Vol. 127, Issue

19, pp. 4111–4122). https://doi.org/10.1242/jcs.151753

Wang, Y., Wei, J.-H., Bisel, B., Tang, D., Seemann, J., Marsh, B., Volkmann, N., McIntosh, J., Howell, K., Mironov, A., Beznoussenko, G., Polishchuk, R., Trucco, A., Trucco, A., Polishchuk, R., Martella, O., Pentima, A. Di, Fusella, A., Elsner, M., … Dirac-Svejstrup, B. (2008). Golgi Cisternal Unstacking Stimulates COPI Vesicle Budding and Protein Transport. *PLoS ONE*, *3*(2), e1647. https://doi.org/10.1371/journal.pone.0001647

Wei, J.-H., & Seemann, J. (2009). The mitotic spindle mediates inheritance of the Golgi ribbon structure. *The Journal of Cell Biology*, *184*(3), 391–397. https://doi.org/10.1083/jcb.200809090

Wei, J.-H., Zhang, Z. C., Wynn, R. M., & Seemann, J. (2015). GM130 Regulates Golgi-Derived Spindle Assembly by Activating TPX2 and Capturing Microtubules Article GM130 Regulates Golgi-Derived Spindle Assembly by Activating TPX2 and Capturing Microtubules. *Cell*, *162*, 287–299. https://doi.org/10.1016/j.cell.2015.06.014

Weisz, O. A., & Rodriguez-Boulan, E. (2009). Apical trafficking in epithelial cells: Signals, clusters and motors. In *Journal of Cell Science* (Vol. 122, Issue 23, pp. 4253–4266). https://doi.org/10.1242/jcs.032615

Welgert, R., Silletta, M. G., Spanò, S., Turacchie, G., Cericola, C., Colanzi, A., Senatore, S., Mancini, R., Pollshchuk, E. V., Salmona, M., Facchiano, F., Burger, K. N. J., Mironov, A., Luini, A., & Corda, D. (1999). CtBP/BARS induces fission of Golgi membranes by acylating lysophosphatidic acid. *Nature*, *402*(6760), 429–433. https://doi.org/10.1038/46587

Welsh, C. F., Roovers, K., Villanueva, J., Liu, Y. Q., Schwartz, M. A., & Assoian, R. K. (2001). Timing of cyclin D1 expression within G1 phase is controlled by Rho. *Nature Cell Biology*, *3*(11), 950–957. https://doi.org/10.1038/ncb1101-950

Welte, M. A. (2004). Bidirectional Transport along Microtubules. *Current Biology*, *14*(13), R525–R537. https://doi.org/10.1016/j.cub.2004.06.045

Wong, Y. L., Anzola, J. V, Davis, R. L., Yoon, M., Motamedi, A., Kroll, A., Seo, C. P., Hsia, J. E.,

Kim, S. K., Mitchell, J. W., Mitchell, B. J., Desai, A., Gahman, T. C., Shiau, A. K., & Oegema, K. (2015). Reversible centriole depletion with an inhibitor of Polo-like kinase 4. *Science*, *348*(6239), 1155–1160. https://doi.org/10.1126/science.aaa5111

Woodrum, D. T., Rich, S. A., & Pollard, T. D. (1975). Evidence for biased bidirectional polymerization of actin filaments using heavy meromyosin prepared by an improved method. *Journal of Cell Biology*, *67*(1), 231–237. https://doi.org/10.1083/jcb.67.1.231

Xu, Y., Takeda, S., Nakata, T., Noda, Y., Tanaka, Y., & Hirokawa, N. (2002). Role of KIFC3 motor protein in Golgi positioning and integration. *The Journal of Cell Biology*, *0729311*(2), 21–9525. https://doi.org/10.1083/jcb.200202058

Yadav, S., Puri, S., & Linstedt, A. D. (2009). A Primary Role for Golgi Positioning in Directed Secretion, Cell Polarity, and Wound Healing. *Molecular Biology of the Cell*, *20*, 1728–1736. https://doi.org/10.1091/mbc.E08

Yadav, S., Puthenveedu, M. A., & Linstedt, A. D. (2012a). Golgin160 Recruits the Dynein Motor to Position the Golgi Apparatus. *Developmental Cell*, *23*, 153–165. https://doi.org/10.1016/j.devcel.2012.05.023

Yadav, S., Puthenveedu, M. A., & Linstedt, A. D. (2012b). Golgin160 Recruits the Dynein Motor to Position the Golgi Apparatus. *Developmental Cell*, *23*(1), 153–165. https://doi.org/10.1016/j.devcel.2012.05.023

Yang, C., Czech, L., Gerboth, S., Kojima, S. I., Scita, G., & Svitkina, T. (2007). Novel roles of formin mDia2 in lamellipodia and filopodia formation in motile cells. *PLoS Biology*, *5*(11), 2624–2645. https://doi.org/10.1371/journal.pbio.0050317

Zhang, X., & Wang, Y. (2016). GRASPs in Golgi structure and function. In *Frontiers in Cell and Developmental Biology* (Vol. 3, Issue JAN). Frontiers Media S.A. https://doi.org/10.3389/fcell.2015.00084

Zigmond, S. H. (2004). Beginning and Ending an Actin Filament: Control at the Barbed End. In *Current Topics in Developmental Biology* (Vol. 63). https://doi.org/10.1016/S0070-

2153(04)63005-5